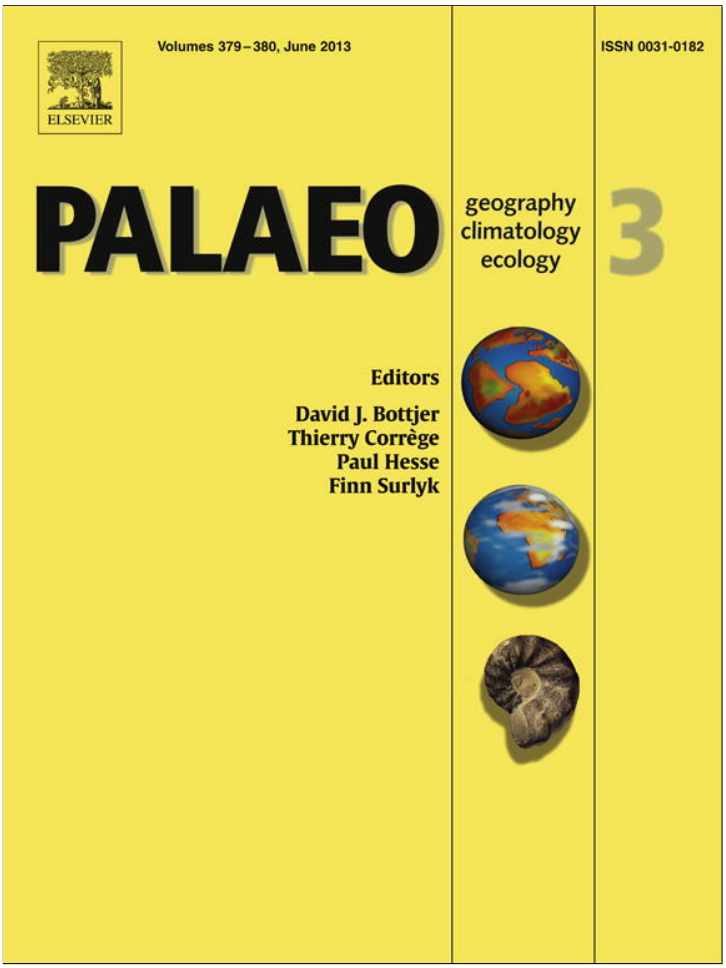

Palaeogeography, Palaeoclimatology, Palaeoecology 379–380 (2013) 39–53

Contents lists available at SciVerse ScienceDirect

Palaeogeography, Palaeoclimatology, Palaeoecology

journal homepage: www.elsevier.com/locate/palaeo

Paleoclimate changes of the last 1000 yr on the eastern Qinghai–Tibetan Plateau recorded by elemental, isotopic, and molecular organic matter proxies in sediment from glacial Lake Ximencuo

Yang Pu [a,*], Trevor Nace [b], Philip A. Meyers [c], Hucai Zhang [d], Yongli Wang [e], Chuanlun L. Zhang [f], Xiaohua Shao [a]

[a] School of Remote Sensing, Nanjing University of Information Science & Technology, Nanjing 210044, China
[b] Duke University, Division of Earth and Ocean Sciences, Durham, NC 27708-0227, USA
[c] Department of Earth and Environmental Sciences, The University of Michigan, Ann Arbor, MI, 48109-1005, USA
[d] Key Laboratory of Plateau Lake Ecology and Global Change, Yunnan Normal University, Kunming Chenggong 650500, China
[e] Key Laboratory of Petroleum Resources Research, Institute of Geology and Geophysics, Chinese Academy of Sciences, Lanzhou 730000, China
[f] Department of Marine Sciences, The University of Georgia, Athens, GA 30602, USA

ARTICLE INFO

Article history:
Received 25 July 2012
Received in revised form 2 March 2013
Accepted 24 March 2013
Available online 10 April 2013

Keywords:
Biomarker
n-Alkane
n-Alkan-ol
Organic carbon and nitrogen isotopes
Qinghai–Tibetan Plateau
Suess Effect

ABSTRACT

Total organic carbon (C_{org}) and nitrogen (N_{tot}) concentrations and isotope compositions and *n*-alkane and *n*-alkan-ol molecular biomarker compositions were measured in two parallel sediment cores from Lake Ximencuo, a typical glacial lake on the eastern Qinghai–Tibetan Plateau (QTP), to reconstruct local climatic variations during the past 1000 yr. Concentrations of C_{org} and N_{tot} vary similarly with changes in precipitation recorded by tree rings in Dulan, northeastern QTP, indicating their close relation to precipitation. Carbon Preference Index (*CPI*) values of C_{22}–C_{33} *n*-alkanes and C_{22}–C_{28} *n*-alkan-1-ols and Average Chain Length (*ACL*) values of C_{27}–C_{33} *n*-alkanes generally negatively correlate with $\delta^{13}C_{org}$ and $\delta^{15}N_{tot}$ and also vary comparably with the oxygen isotope temperature record from the Dunde ice core, northeastern QTP. These patterns indicate that high *CPI* values and negative shifts of the $\delta^{13}C_{org}$ and $\delta^{15}N_{tot}$ correspond to warmer conditions that favor the growth of vascular land plants and that lower values and positive shifts correspond to cooler conditions in the Lake Ximencuo locality. This observation contradicts previous interpretations from peat and modern soil studies that conclude that the *CPI* indices were controlled by microbial degradation under different climate conditions. Here we propose that the changes of organic matter sources under different climate regimes, combined with physiological adjustments of vascular plants to different air temperatures, might yield different *CPI* responses to climate changes in glacial plateau lakes. Air temperature and precipitation increases and decreases reconstructed in this 1000-yr study were generally independent of each other, but they both occurred at centennial or multi-centennial scales. The interaction between subtropical (Asian Monsoon) and mid-latitude (Westerly) atmospheric circulation systems probably dominated the local precipitation variations in the Lake Ximencuo catchment, whereas solar insolation, volcanism and greenhouse gas variations were likely responsible for the air temperature changes that are recorded in the lake sediments and that are consistent with regional temperature variations in the eastern QTP.

1. Introduction

The Qinghai–Tibetan Plateau (QTP) is the largest elevated landmass in the world and strongly influences major features of Asian atmospheric circulation, including the East Asian Monsoon, the Indian Monsoon, and the Westerlies (An et al., 2001). Paleoclimatic and environmental reconstructions on the QTP can improve predictions of future changes in monsoon dynamics and their ecological impacts by yielding a perspective on past changes in climate in this region. In particular, the climate evolution of the past millennium, which is a period of significant climate variations, including the Medieval Warm Period (*MWP*), the Little Ice Age (*LIA*) and Modern Warming (*MW*), is particularly important because it helps to evaluate the impact of the global warming trend of the past century against the longer natural climate change background.

Studies have explored the paleoclimate history of the QTP using various natural archives, including ice cores (e.g. Thompson et al., 1989; Yao et al., 1996; Thompson et al., 1997; Yao et al., 1997), tree rings (e.g. Sheppard et al., 2004; Shao et al., 2005; Zhu et al., 2011), lacustrine sediments (e.g. Shen et al., 2005; Wu et al., 2006, 2007; Henderson and Holmes, 2009; Aichner et al., 2012), and peat

* Corresponding author. Tel.: +86 25 84372740; fax: +86 25 5869 5671.
E-mail address: puyangnew@126.com (Y. Pu).

0031-0182/$ – see front matter © 2013 Elsevier B.V. All rights reserved.
http://dx.doi.org/10.1016/j.palaeo.2013.03.023

sequences (e.g. Zhou et al., 2010; Zheng et al., 2011a,b). Among these, lacustrine sediment sequences have been most frequently used because of the numerous lakes distributed in this vast high plateau that serve as recorders for paleoclimate reconstructions. In addition, the plateau lakes are usually characterized by stable sedimentary environments with little human disturbance. However, previous researchers have focused primarily on large, tectonically derived lakes, such as Lake Qinghai (e.g. Ji et al., 2005; Shen et al., 2005) and Nam Co (e.g. Mügler et al., 2008; Zhu et al., 2008) because they are considered to provide longer and larger regional climatic signals. In contrast, many small glacial lakes that are broadly distributed in the QTP have been rarely used in paleoclimate and paleoenvironment studies (Wang and Dou, 1998). This type of lake commonly exists in cirques or trough valleys that are characterized by steep slopes that encourage land runoff. Therefore, both glacial meltwater and local precipitation have a strong scouring effect on the slope vegetation and soil, transporting large amounts of terrigenous material into the lake. In addition, because of the relatively deep water of these steep-sided lakes, the sedimentary environment is very stable, and consequently the sediment record tends to be little disturbed and its organic matter well preserved.

Compositional changes in the organic matter buried over time in lake sediments can provide special insights into the history of a lake and its catchment. Organic matter abundance, isotopic composition, and molecular biomarker content have been integrated to reconstruct paleoclimatic and paleoenvironmental conditions in several QTP lakes (e.g. Herzschuh et al., 2005; Lin et al., 2008; Aichner et al., 2012). Bulk organic matter in lake sediment is derived from plants and organisms living in the lake and its watershed and consequently contains an integrated signal that reflects the collective paleoclimate and paleoenvironmental variations (Meyers, 2003). Moreover, lipid molecular biomarkers are often more sensitive to climatic change than bulk organic matter or the pollen and spores that are based on morphology (Xie and Evershed, 2001). However, the multiple sources and post-depositional microbial degradation of the biomarkers in a lake system sometimes complicate interpretations of the proxies. It also remains uncertain about how different paleolimnological records derived from separate biomarker and bulk organic matter proxies can be reconciled to better understand changes in lake system. These problems can limit the application of biomarker studies and bulk organic geochemical properties in paleoclimatic and paleoenvironmental reconstructions, but they can potentially be resolved by study of multiple proxies on the same samples.

Here, we apply bulk organic matter proxies ($\%C_{org}$, $\%N_{tot}$, C/N, $\delta^{13}C_{org}$ and $\delta^{15}N_{tot}$) in combination with lipid biomarker proxies (*n*-alkane and *n*-alkan-ol *CPI* and *ACL* values) from Lake Ximencuo sediments deposited over the past ca. 1000 yr to investigate the potential relations between different organic indexes and to try to reconstruct the paleoclimatic and related paleoenvironmental variations. Furthermore, we compare the organic geochemical proxy record from this study with the high-resolution ice core $\delta^{18}O$ temperature record and tree-ring precipitation record in the eastern part of the QTP to relate the local changes to regional climate evolution.

2. Material and methods

2.1. Study area

Nianbaoyeze Mountain (32°58′ to 33°22′ N, 100°59′ to 101°20′ E), which is located in Jiuzhi, Qinghai Province, is a granite dome on the eastern Tibetan Plateau, and its highest peak is still covered by glaciers (Lehmkuhl, 1998). The weather in this region is influenced by several atmospheric systems, including the Indian Summer Monsoon (ISM), the East Asian Summer Monsoon (EASM) and the Westerlies (Fig. 1), which create a more complex climate system compared to other parts of the QTP. Most of the precipitation comes from the Indian Ocean and Pacific Ocean via the summer monsoons. Meteorological data show that this region has the highest precipitation within Qinghai Province, with an average of 774 mm, and an annual evaporation of a little less than 1250 mm; more than 80% of the annual precipitation falls during May to October. The mean annual temperature is about 0.1 °C, and the annual sunshine totals 2084.5–2509.5 h (China Meteorological Data Sharing Service System). The low temperature and relatively short sunshine hours result in the lake being ice-covered for four to five months every winter season.

Lake Ximencuo is a typical glacial lake in the Nianbaoyeze Mountain area, having been formed behind a terminal moraine by melt water from the Nianbaoyeze glacier in the post-glacial period (Zhang and Mischke, 2009). The modern glacier still feeds the lake via small streams. The lake basin is relatively long and narrow (Fig. 1), and both sides are steep, but the ends have gentle slopes. This shape reflects glacial advance and retreat within the basin valley; most of the glacial lakes in the region have similar morphologies. The average elevation of the lake surface is 4020 m, and its area is 3.8 km^2. The average depth of Lake Ximencuo is approximately 40 m, with the maximum depth close to 65 m, although the lake level commonly varies by a few meters between wet and dry seasons.

Several geochemical studies leading to climatic and environmental reconstructions of the eastern QTP were conducted in Lake Ximencuo in the early 1990s. A core of 1.47 m length, which captured 2000 yr of sedimentary history, was taken in the northern bay of the lake by a research group from Nanjing Institute of Geography and Limnology, Chinese Academy of Sciences, and was subsequently studied using organic carbon isotopes, pigments, magnetic properties, and pollen and spores (Yang, 1996; Wang et al., 1997; Xue et al., 1997). The pollen studies suggest that vegetation for the last two millennia in the study area has been dominated by herbaceous and shrubby plants including Cyperaceae, Gramineae, *Artemisia* and Rossaceae (Yang, 1996). Subsequently, Zhang and Mischke (2009) reconstructed the lake evolution history and corresponding climate conditions for the past 19 kyr by means of magnetic susceptibility, grain-size analysis, and major and trace elements in a 12.81 m core from a water depth of 56 m near the middle of the lake. They concluded that Lake Ximencuo has been a permanently deep lake without any important geological or structural disturbances throughout its history since the Last Glacial Maximum.

2.2. Sediment sampling and lake water measurements

Two parallel cores were taken at a water depth of 34.4 m in Lake Ximencuo using a gravity corer at a GPS location of 33°22′40.59″ N, 101°06′21.78″ E in July, 2009. The sediment sequences were a light gray color with a silty clay texture and had no obvious alterations or unconformities. One core (XMC-5) was 51 cm long and was subsampled every 0.5 cm down to 20 cm and then every 1 cm to the bottom of the core for bulk organic matter analysis in the Duke University Environmental Stable Isotope Laboratory and for ^{210}Pb and ^{137}Cs dating measurements at East Carolina University. The other core (XMC-6) was 44 cm long and was subsampled in 2 cm increments for lipid biomarker studies in the China University of Geosciences (Wuhan). Samples were wrapped in foil, put in a sample bag and preserved in a freezer (−20 °C) until analysis.

Water chemistry and physical properties were analyzed for the surface water close to the core site using a YSI 6600 multi-parameter water quality monitor (Table 1). The temperature in the surface water was about 13 to 14 °C during sample collection. The pH value was about 8.9, recording a weakly alkaline water environment. The surface chlorophyll level was 30.0 μg/L, suggesting high primary productivity, which may have resulted in significant organic carbon export from phytoplankton to the lake sediments. Total Dissolved Solids (TDS) concentration was about 44 mg/L, which is in the range of the global average rainfall water TDS of 20–50 mg/L (Shen et al., 1993) and is much lower than the average TDS values of surface water in Qinghai lake

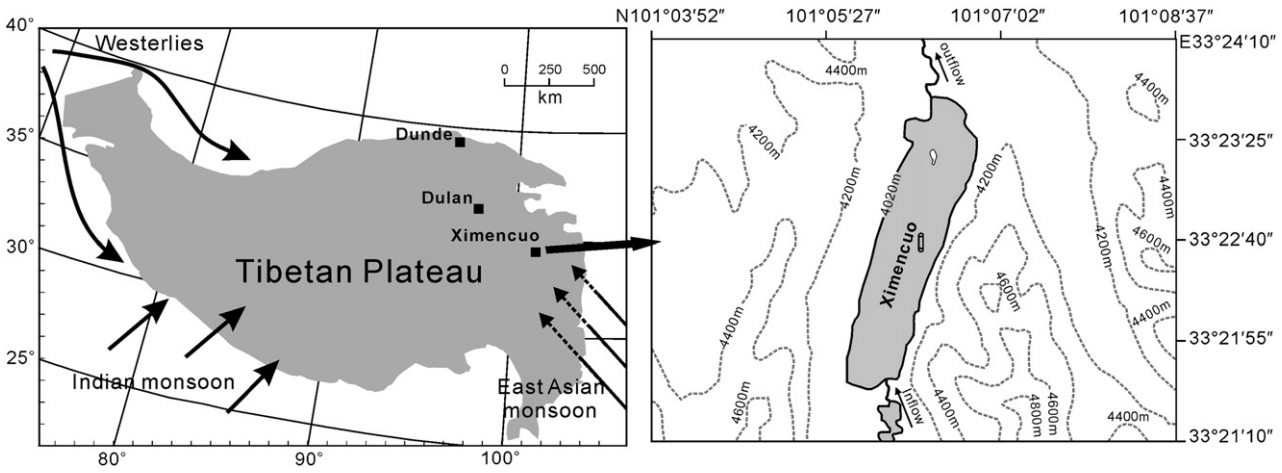

Fig. 1. Study area of Lake Ximencuo on the eastern QTP and a picture of Lake Ximencuo where the drilling site is marked out.

(Xu et al., 2010) and Nam Co (Wrozyna et al., 2011), which are both terminal lakes. The low TDS confirm a fresh water environment in Lake Ximencuo, which is a flow-through lake (Fig. 1).

2.3. Sediment dating

The sedimentation rate at the core site was estimated from ^{210}Pb and ^{137}Cs measurements done in the Department of Geological Sciences at East Carolina University (Table 2 and Fig. 2). Samples were taken at 1 cm intervals, dried at 60 °C, pulverized, packed into standardized vessels and sealed for greater than 24 h before counting commenced. Samples were analyzed by direct gamma counting on a germanium detector that was calibrated using a natural matrix standard (IAEA-300). Excess ^{210}Pb activities were determined by subtracting total ^{210}Pb (46.5 keV) from that given by ^{226}Ra. ^{226}Ra was determined indirectly by counting the gamma emissions of its granddaughters, ^{214}Pb (295 and 351 keV) and ^{214}Bi (609 keV).

The AMS ^{14}C results of Mischke and Zhang (2010) indicate that sediment accumulation rates in deep-water areas of Lake Ximencuo have been basically constant for at least the last two millennia. Therefore, the constant initial concentration model of Appleby and Oldfield (1992), which assumes a constant sedimentation rate, was used to calculate the ^{210}Pb time series of the Core XMC-5. Based on the average sedimentation rate of 0.5 mm/yr, the bottom of Core XMC-5 was dated to ca. 900 yr BP and the bottom of Core XMC-6 was dated to ca. 1000 yr BP. The chronological framework was established by this sedimentation rate for the two cores.

To test our time scale, ^{14}C dating was performed at the National Ocean Sciences Accelerator Mass Spectrometry Facility (NOSAMS), Woods Hole Oceanographic Institute, to assess whether the ^{210}Pb chronological framework is reasonable. Owing to a lack of ideal dating materials, such as animal remains, terrestrial plant macrofossils, or charcoal, in the Lake Ximencuo sediments, we used bulk organic matter from the bottom centimeter of Core XMC-5 (50–51 cm) for the radiocarbon dating. An age of 3431 cal yr BP with an error of 30 cal yr was obtained, and this result is unreasonably older than the ^{210}Pb and ^{137}Cs measurements and even older than the AMS age at the same core depth from Mischke and Zhang (2010). A possible explanation for this discrepancy is that the ^{14}C ages obtained from measurements on bulk organic carbon can be affected by the reservoir effect, which can be large in small lakes because of soil-derived carbon. This phenomenon is particularly common in the radiocarbon dating of sediments in the QTP lakes, which have carbon reservoir ages ranging from hundreds to thousands of years (Liu et al., 2008). In this study, it is hard to determine the surface reservoir age of the Lake Ximencuo from the limited radiocarbon data, so we elected to discard the age obtained from the ^{14}C dating and to use the sedimentation rate estimated from the ^{210}Pb and ^{137}Cs data.

2.4. Organic geochemical measurements

Sediment samples were treated with HCl to remove inorganic carbon in preparation for analyses of $\delta^{13}C_{org}$, $\delta^{15}N_{tot}$, $\%C_{org}$ and $\%N_{tot}$. Between 9 and 12 mg of the carbonate-free sediment was placed in tin capsules and analyzed using a Thermo Finnigan MAT 253 isotope ratio mass spectrometer coupled with a flash elemental analyzer. The isotopic measurement precision based on our laboratory standards (urea and glycine), which were calibrated against International Atomic Energy Agency standards, was approximately 0.15‰ and 0.3‰ for $\delta^{13}C_{org}$ and $\delta^{15}N_{tot}$, respectively.

The frozen samples for lipid analysis were immediately freeze-dried upon arrival at the laboratory in Nanjing. A subsample of approximately 2 g was passed through a number 80 mesh sieve to eliminate any large pieces of biological debris. The soluble lipid content of the organic matter was released by ultrasonic extraction

Table 1
Surface water properties close to the core site in the Lake Ximencuo.

Depth (cm)	13.6
Temperature(°C)	13.28
pH	8.89
Turbidity (NTU)	2.8
Chlorophyll-a (μg/L)	30.3
Conductivity (mS/cm)	0.053
Dissolved oxygen (%)	4.9
Resistivity (kΩ·cm)	19.02
TDS (mg/L)	44

Table 2
Summary of the $^{210}Pb_{tot}$, $^{210}Pb_{exc}$ and ^{137}Cs radiochronological data.

Depth (cm)	$^{210}Pb_{tot}$ (dpm/g)		$^{210}Pb_{exc}$ (dpm/g)		^{137}Cs (dpm/g)	
	Activity	Err (±)	Activity	Err (±)	Activity	Err (±)
0–1	75.59	8.73	70.94	8.74	6.31	0.41
1–2	44.52	5.56	40.07	5.58	8.28	0.34
2–3	33.58	4.50	28.81	4.54	4.48	0.27
3–4	13.09	4.22	7.76	4.22	2.41	0.31
4–5	10.83	3.50	5.62	3.54	0.93	0.24
5–6	8.25	2.14	4.19	2.18	0.45	0.14
6–7	3.78	1.76	0.06	1.89	0.05	0.12
7–8	2.78	1.38	−1.48	1.39	0.00	0.00
8–9	5.67	2.35	0.47	2.51	0.00	0.15

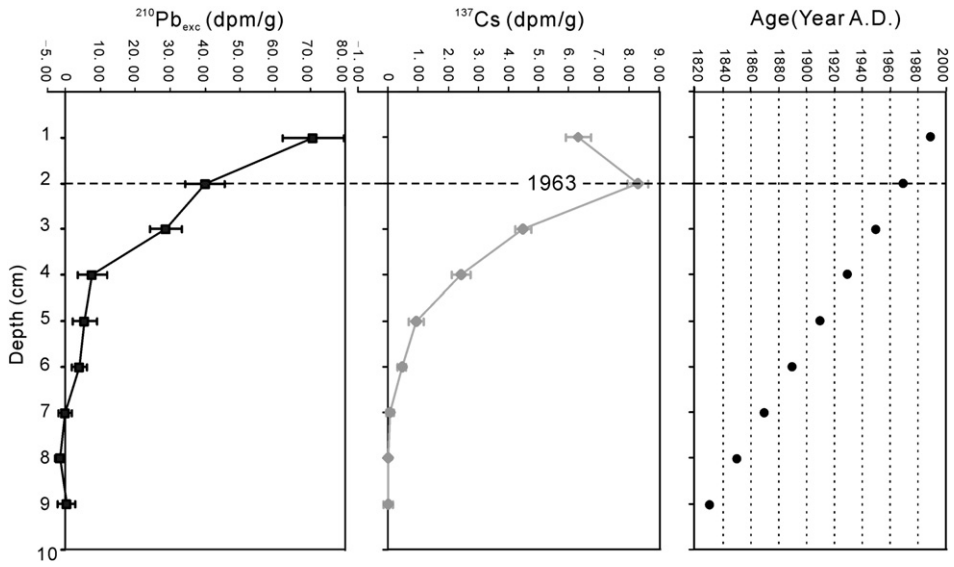

Fig. 2. Excess ^{210}Pb activity and total ^{137}Cs activity in dpm/g. The age model is a log-linear regression (constant initial concentration (CIC) model).

(3×) with solvent (dichloromethane/methanol, 93/7) for 20 min using an ultrasonic generator. The three extracts were combined, filtered, and then concentrated to constant weight. After being air dried, the extracts were derivatized by heating with N, O-bis (trimethylsilyl) trifluoroacetamide to prepare them for GC/MS analysis.

GC–MS was performed with a Hewlett Packard 7890A gas chromatograph interfaced with a Hewlett Packard 5975C mass selective detector and equipped with a DB-5 MS column (30 m × 0.25 mm ID, film thickness 0.25 μm). The oven temperature was gradually increased from 70 to 300 °C (held 20 min) at 3 °C/min. Helium was used as a carrier gas. Identifications of individual *n*-alkanes and *n*-alkan-1-ols were done by comparison with mass spectra and retention times from the literature, and the area normalization method was used to quantify individual components.

3. Organic geochemical results and general interpretations

Reconstruction of the 1000 yr record paleoclimate changes from Lake Ximencuo is based on our multiproxy elemental, isotopic, and molecular analyses of sediment organic matter. Below we briefly summarize the primary controls on each of these proxies, and then we discuss their linked interpretations.

3.1. Bulk elemental records in Lake Ximencuo

C_{org} concentrations vary between 3.6 and 5.9%, and those of N_{tot} are between 0.3 and 0.7%; both parameters have similar patterns in the sediment record (Fig. 3a and b). The concentrations exhibit relatively stable trends from 51 to 10 cm with an average of 4.4% for C_{org} and 0.49% for N_{tot}, respectively, except for two obviously lower values at the depths of 48 cm and 34 cm. From 10 cm to the top of the core, the percentages first decrease abruptly, almost reaching their lowest values, followed by a rapid increase from 8 cm to the top of the core. The two concentrations have a significant positive correlation ($r = 0.91$, $\alpha = 0.01$, 2-tailed) whereas both of them showed relatively low correlation coefficients with $\delta^{13}C_{org}$ and $\delta^{15}N_{tot}$, respectively. It is likely that the major factors that are responsible for the $\%C_{org}$ and $\%N_{tot}$ variation as well as the $\delta^{13}C_{org}$ and $\delta^{15}N_{tot}$ variation are very different. Also noteworthy is neither $\%C_{org}$ nor $\%N_{tot}$ shows a downcore decreasing trend in Core XMC-5, indicating that degradation seems to be minor during the process of accumulation. Therefore, organic matter paleoenvironmental signals of these two proxies should be well preserved.

3.2. Atomic C_{org}/N_{tot} ratios

C_{org}/N_{org} is a general proxy that can be used to approximate the relative contributions of allochthonous and autochthonous organic matter to lake sediments. It is calculated from the measured concentrations of organic carbon and nitrogen. Because the concentration of N often contains both organic nitrogen and inorganic nitrogen, the C_{org}/N_{tot} is likely to be smaller than the C_{org}/N_{org} ratio. However, a cross-plot of the two concentrations yields a positive carbon intercept (Fig. 4a), which indicates that inorganic N contributes little or nothing to the total N concentrations in these sediments (Calvert, 2004). We speculate that the "extra" carbon may be recycled from ancient organic carbon in the rock flour that is characteristic of glacial lakes. Hence, we use the C_{org}/N_{tot} instead of the C_{org}/N_{org} ratio as a proxy for the origin of the organic matter in these sediments.

In Core XMC-5, the atomic C_{org}/N_{tot} ratio ranges from 9.7 to 14.2 with a mean value of 10.7. Worth pointing out is that the C_{org}/N_{tot} ratio is fairly uniform throughout the profile except for a dramatic rise from about 6 cm to 9 cm that is centered on 7.5 cm (Fig. 3c). This interval also has low concentrations of C_{org} and N_{tot}. Previous studies have shown that aquatic algae have atomic C_{org}/N_{org} ratios <10, submerged and floating aquatic macrophytes or organic matter of a mixed source have C_{org}/N_{org} ratios between 10 and 20, whereas emersed and terrestrial plants have C_{org}/N_{org} ratios >20 (Meyers, 2003, and references therein). Thus, it appears that the 6–9 cm dramatic rise of C_{org}/N_{tot} ratio and the corresponding low concentrations of C_{org} and N_{tot} might result from an episodic increase in wash-in of terrestrial material and an associated decrease in primary productivity in Lake Ximencuo.

3.3. Carbon and nitrogen isotopes of bulk organic matter

The $\delta^{13}C_{org}$ values of the lake sediments vary between −24.4‰ and −23.1‰ with an average of −23.6‰ (Fig. 3d), and the $\delta^{15}N_{tot}$ values vary between 2.8‰ and 4.3‰ with an average value of 3.9‰ (Fig. 3e). Both parameters vary within a relatively small range throughout the whole core and show comparable trends, suggesting that they may be controlled by similar limnological factors in this study.

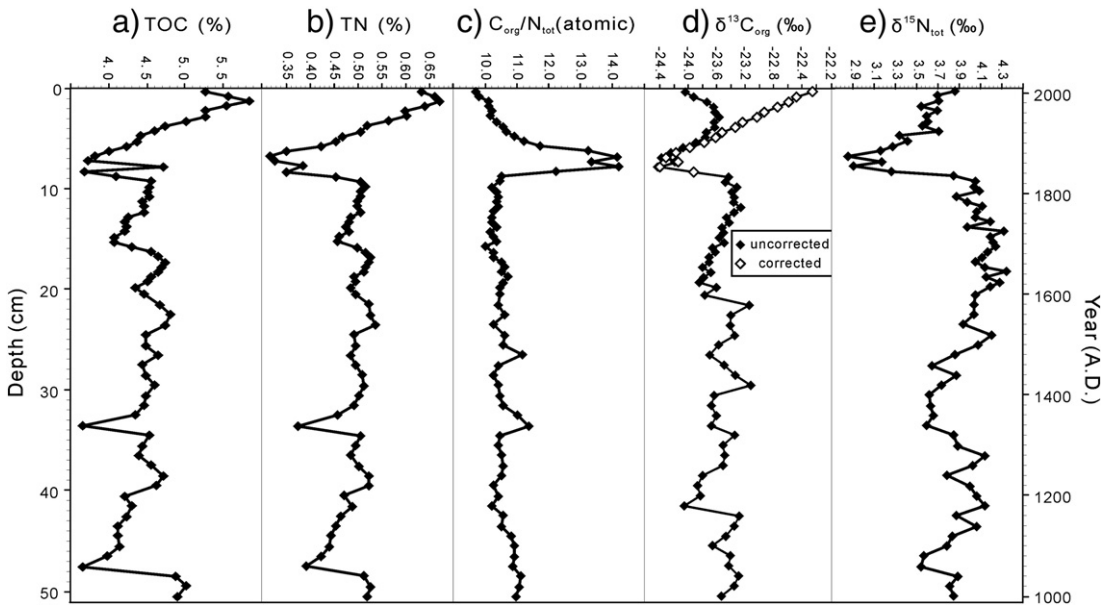

Fig. 3. Vertical profiles of the bulk organic matter proxies of $\%C_{org}$, $\%N_{tot}$, C_{org}/N_{tot} (atomic), $\delta^{13}C_{org}$ and $\delta^{15}N_{tot}$ in Core XMC-5. Corrections for the Suess Effect since AD 1840 based on the equation provided by Schelske and Hodell (1995).

However, $\%C_{org}$ and $\%N_{tot}$ increased significantly in the last century, and C/N ratios decrease in the corresponding period. These changes are indicators of a likely increase in lake productivity (Meyers, 2003), which might have been caused by the paleoenvironmental changes in this study. If productivity increased, the $\delta^{13}C_{org}$ values should become less negative, but they become more negative since about 1950 AD. This pattern really looks as the Suess Effect — the shift to more negative $\delta^{13}C$ values of atmospheric CO_2 caused by fossil fuel combustion and deforestation — has biased the isotope signal (Keeling, 1979). We tentatively applied the equation as provided by Schelske and Hodell (1995) to correct the $\delta^{13}C_{org}$ values since AD 1840, where Y is time (in yr):

$$\delta^{13}C_{atm} = 4577.8 - 7.3430 * Y + 3.9213 * 10^{-3} * Y^2 - 6.9812 * 10^{-7} * Y^3 \quad (Y \geq 1840).$$

The overall Suess Effect $\delta^{13}C$ depletion is about −1.99‰ from AD 1840 to 2009, and the calculated time-dependent depletion in $\delta^{13}C$ value was subtracted from the $\delta^{13}C$ values in samples since AD 1840. The corrected $\delta^{13}C_{org}$ values show a less negative excursion in the last century that reaches −22.3‰ showing the highest value in the $\delta^{13}C_{org}$ curve. Only when the values are corrected for the Suess Effect do they agree with the increase in primary productivity indicated by the $\%C_{org}$, $\%N_{tot}$ and C/N proxies. Thus, we decided to use the Suess-corrected $\delta^{13}C_{org}$ values from AD 1840 instead of uncorrected ones to discuss the paleoenvironmental variations in the following sections.

3.4. Distributions of n-alkan-1-ols and n-alkanes and their derived proxies

We identified several series of lipid biomarkers in Ximencuo Lake sediments, including *n*-alkanes, *n*-alkenes, *n*-alkan-1-ols, *n*-alkan-2-ones, fatty acids, terpenoids, and sterols. However, the most abundant compound classes are the *n*-alkan-1-ols (*n*-alkan-ols hereafter) and *n*-alkanes, which make up 19.7%–51.5% and 8.7%–18.9% of the extractable lipid matter, respectively. In virtually all plant waxes, long chain *n*-alkan-ols and *n*-alkanes are abundant and can account for more than 60% of the epicuticular lipids (Tulloch, 1976). Generally, the lipid biomarker series having higher abundances should yield more reliable results than less abundant ones because their analytical errors would be proportionally smaller. Moreover, both *n*-alkan-ols and *n*-alkanes

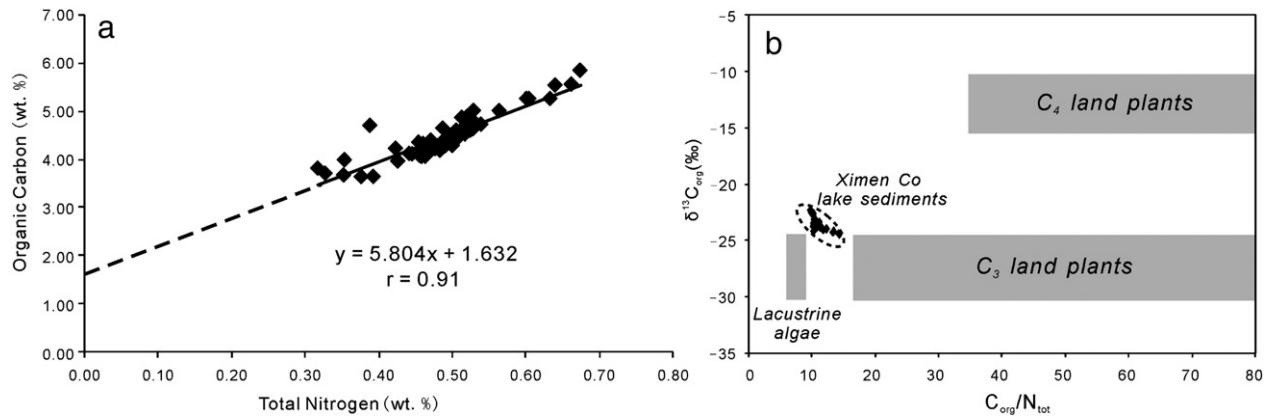

Fig. 4. (a) the cross-plot of the C_{org} and N_{tot} concentrations in the Core XMC-5; (b) $\delta^{13}C_{org}$, with values corrected for the Suess Effect since AD 1840, and atomic C_{org}/N_{tot} values of Lake Ximencuo sediments relative to generalized compositions of organic matter from lacustrine algae, C_3 land plants, and C_4 land plants (Meyers, 2003).

are relatively more resistant to biodegradation than other organic matter components and are consequently better preserved in lake sediments (Eglinton and Eglinton, 2008). Consequently, only the *n*-alkan-ol and *n*-alkane distributions were investigated for their potential paleoclimatic significance in this study.

Because they are generally considered more durable than *n*-alkan-ols in sedimentary settings, we first discuss the *n*-alkanes in the Ximencuo sediments. Their carbon chain-lengths range from *n*-C_{15} to *n*-C_{33} and have a unimodal distribution (Fig. 5). The long-chain *n*-alkanes (*n*-C_{22}–*n*-C_{33}) comprise more than 90% of the total *n*-alkane abundance and are characterized by a pronounced odd-carbon predominance. These compounds are generally considered to be derived from the leaf waxes of vascular plants, including submerged, floating and emersed aquatic plants and terrestrial higher plants (Eglinton and Hamilton, 1967; Ficken et al., 2000). Previous studies have shown that plants in the Ximencuo region are dominated by herbs and shrubs, with their pollen comprising more than 90% of the total pollen concentration (Yang, 1996). Therefore, the higher vegetation characteristics deduced from the *n*-alkane distribution are consistent with the pollen results. In contrast to the relatively abundant long-chain components, the short-chain-length *n*-alkanes are at low to undetectable concentrations without any odd/even predominance. We infer that they mainly originate from algae, cyanobacteria, fungi, and microbes living in the lake environment (Cranwell et al., 1987; Meyers, 1997).

The chain-length distributions of the Ximencuo *n*-alkan-ols are from *n*-C_{13} to *n*-C_{32} and are dominated by long-chain components in the *n*-C_{22} to *n*-C_{28} range (Fig. 6). An obvious even/odd carbon number predominance was seen for chain-lengths greater than 22 throughout all samples, indicating they are well preserved with minor degradation. Although *n*-alkan-ols cannot be used as a diagnostic biomarker to indicate a specific organism, different kinds of biota usually have different distribution patterns. For instance, lipids from aquatic algae and photosynthetic bacteria have large proportions of the C_{16} to C_{22} *n*-alkan-ols (Robinson et al., 1984; Volkman et al., 1998); submerged and floating plants are dominated by C_{22} or C_{24} *n*-alkan-1-ols (Ficken et al., 1998); land plant and emersed aquatic plants range from C_{22} to C_{28} with strong even/odd predominance (Eglinton and Hamilton, 1967; Rommerskirchen et al., 2006; Vogts et al., 2009).

Carbon Preference Index (*CPI*) values are useful to describe the molecular distributions of aliphatic compounds and have been widely applied in sediment studies for paleoenvironmental reconstruction. However, they are seldom used to reconstruct the paleoenvironment variation in lacustrine sediments because the processes determining this parameter are complicated. Many possible factors, such as diagenetic degradation, microbial alterations, changes in the lipid origins, and climate-induced physiological responses in plants, can potentially influence *CPI* values. Herein, we use the chain-lengths from *n*-C_{21} to *n*-C_{33} for *n*-alkanes ($CPI_{21–33ALK}$) and from *n*-C_{22} to *n*-C_{28} for *n*-alkan-ols ($CPI_{22–28ACH}$) to calculate their *CPI* proxies for paleoclimate discussions because of their notable carbon number predominance and relatively higher abundance than other homologues. The $CPI_{21–33ALK}$ values range from 5.0 to 8.0 and the $CPI_{22–28ACH}$ values range from 4.7 to 10.2; these large values indicate good preservation of these straight-chain biomarkers. The values are relatively high from 44 cm to 24 cm (AD 1130 to 1530) and then decrease abruptly, becoming lower from about 24 cm to 10 cm (AD 1530 to 1820), and then showing exactly the same shifts from 10 cm to 0 cm (AD 1820 to modern) (Fig. 7). The similar trends imply that both parameters are controlled by the same factors.

We also calculated average chain length (*ACL*) values for the *n*-alkanes and *n*-alkan-ols over the chain length ranges of C_{27} to C_{33} ($ACL_{27–33ALK}$) and C_{22} to C_{28} ($ACL_{22–28ACH}$), respectively, which represent the subaerial vascular plant inputs. The climatic significance of the *ACL* is better defined than the *CPI*. It is believed to respond to temperature variations and has been applied as a paleotemperature proxy in a number of studies (e.g. Hughen et al., 2004; Zhang et al., 2006; Sepúlveda et al., 2009). To maintain a plant's moisture balance and to protect its leaf membranes, the leaf epicuticular wax composition of higher plants changes significantly in response to ambient temperature change. In warmer tropical climates, land plants are postulated to biosynthesize longer chain compounds for their waxy coatings, whereas in cooler temperate regions somewhat shorter chain compounds are produced (Poynter et al., 1989). Accordingly, for a specific area, if the vegetation types remain unchanged during the studied time period, changes in the *ACL* are considered to reflect temperature variations. The *ACL* variations of *n*-alkanes and *n*-alkan-ols in Core XMC-6 are shown in Fig. 7. The $ACL_{27–33ALK}$ ranges from 29.4 to 29.9 with an average of 29.7, and the $ACL_{22–28ACH}$ ranges from 24.7 to 25.4 with an average of 25.0. The $ACL_{27–33ALK}$ and $ACL_{22–28ACH}$ values show different downcore trends. From 44 cm to 24 cm (AD 1130 to 1530), $ACL_{27–33ALK}$ has relatively high values, indicating a high temperature period, whereas the $ACL_{22–28ACH}$ exhibits lower or moderate values. It is likely that the *n*-alkan-ols are more susceptible to degradation than the *n*-alkanes, resulting in the long-chain *n*-alkan-ols being somewhat shortened by degradation and thus the $ACL_{22–28ACH}$ values are comparatively lower in the deeper section. From 24 cm to the core top, the $ACL_{22–28ACH}$ shows the same pattern with $ACL_{27–33ALK}$, which indicates that the temperature first decreased from 24 cm to 10 cm (AD 1530 to 1820) and then gradually increased from 10 cm to the top (AD 1820 to modern). The comparable trends between the $ACL_{27–33ALK}$ as well as $CPI_{21–33ALK}$, $CPI_{22–28ACH}$ suggest that the *CPI* indices in Lake Ximencuo are potentially related to past temperature variations.

4. Paleoenvironmental interpretations

4.1. Origins of sedimentary organic matter in Lake Ximencuo sediments

The isotopic compositions of organic carbon and nitrogen are commonly used to assess sources of organic matter and changes in productivity in lakes (Meyers and Lallier-Vergès, 1999). C_4 land plants have an average $\delta^{13}C_{org}$ value of −14‰, while C_3 land plants and lacustrine algae have an average $\delta^{13}C_{org}$ value of −28‰ (Farquhar et al., 1989). $\delta^{15}N_{tot}$ values are about 8.5‰ for algae and about 0.5‰ for C_3 land plants (Meyers, 2003, and references therein). The $\delta^{13}C_{org}$ values, including the Suess corrected ones, in Core XMC-5 are intermediate between the mean characteristic values for C_3 and C_4 vegetation, and $\delta^{15}N_{tot}$ values are intermediate between the mean characteristic values for algae and C_3 vegetation.

The C/N ratio can also be used to assess relative contributions of allochthonous versus autochthonous organic matter (Meyers, 1994). Atomic C/N ratios in Core XMC-5 also suggest that the organic matter in Lake Ximencuo is a mixture of material from different origins including autochthonous aquatic organisms and allochthonous terrestrial plants. By using the dual proxy approach shown in Meyers (2003), we can identify the organic matter sources as shown in Fig. 4b. All Core XMC-5 samples fall between the generalized C/N-$\delta^{13}C_{org}$ compositional fields for algae and terrestrial plants, which is in agreement with any single indicator of $\delta^{13}C_{org}$, $\delta^{15}N_{tot}$ and C/N. Moreover, the samples are closer to the C_3 plants than the C_4 plants, indicating that the vegetation in the Ximencuo catchment is characterized by C_3 plants, which is consistent with the actual flora around this lake (Yang, 1996).

In contrast to the bulk parameter source indicators, the *n*-alkane and *n*-alkan-ol distributions in Core XMC-6 show that their homologous series are dominated by high-carbon-number components that are indicative of considerable higher plant inputs. The biomarkers would seem to indicate that the organic matter is mainly derived from terrestrial and aquatic vascular plants, which contradicts the strongly algal contribution deduced from bulk organic elemental and isotopic compositions. A similar apparent contradiction has

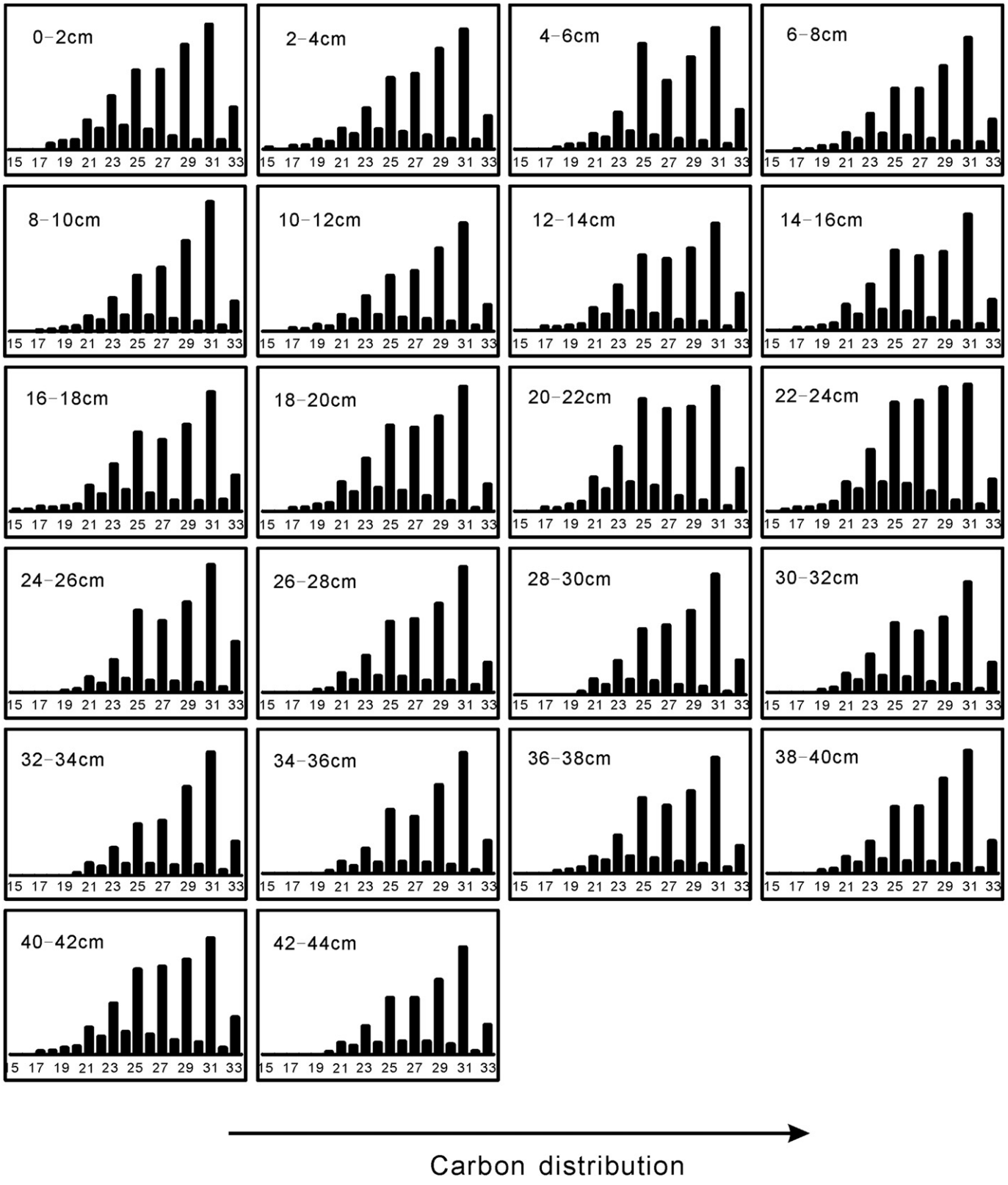

Fig. 5. Relative abundance (vertical) versus carbon distribution (horizontal) of *n*-alkane homologues in Core XMC-6. The carbon number distribution is from C_{15} to C_{33}.

been observed in Lake Wandakara, Uganda, which is a typical crater lake in eastern Africa. The C/N ratio, combined with the $\delta^{13}C_{org}$ values, indicates mixed-source organic matter that is dominated by an algal contribution, but the fatty acid distribution shows strong even/odd chain-length predominance with peak abundances near the C_{30} *n*-acid, indicating primarily terrestrial plant contribution in Lake Wandakara (Russell et al., 2009). Hence, the different types of organic geochemical source proxies seem to present a paradox. Consequently, we argue that the "bulk organic matter origins" are not identical with the "biomarker origins", which have been sometimes confused in

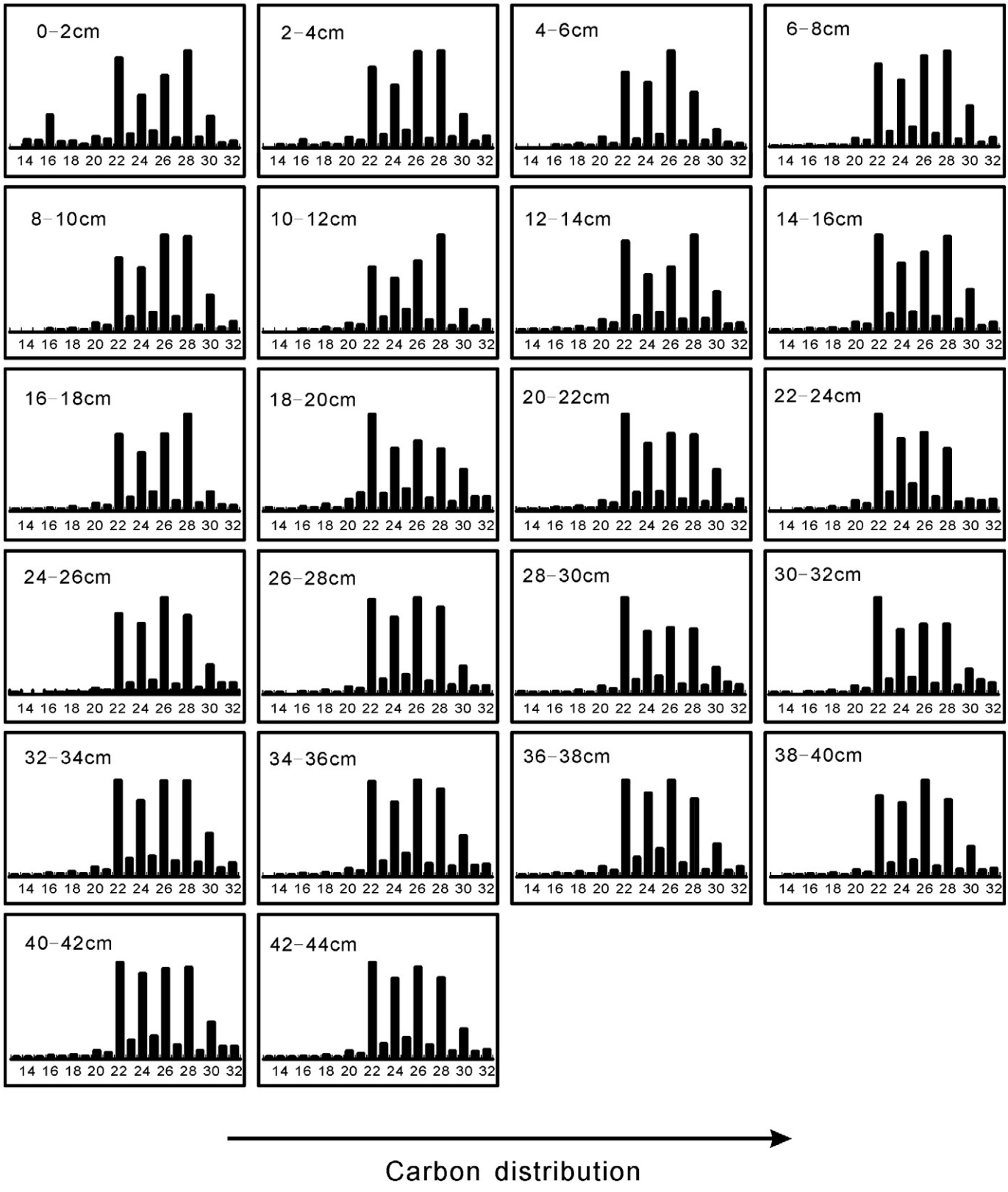

Fig. 6. Relative abundance (vertical) versus carbon distribution (horizontal) of *n*-alkan-ol homologues in Core XMC-6. The carbon number distribution is from C_{13} to C_{32}.

previous studies. This seeming paradox is because lipid biomarkers normally constitute a small fraction of the total organic matter in both biota and sediments (Meyers, 2003) and should not be used to infer the source of total organic matter. We therefore conclude that the multi-proxies derived from the bulk organic matter are more reliable to distinguish the organic matter source, although the biomarker compositions can reveal details of the delivery and deposition of this organic matter. In conclusion, we infer that both autochthonous

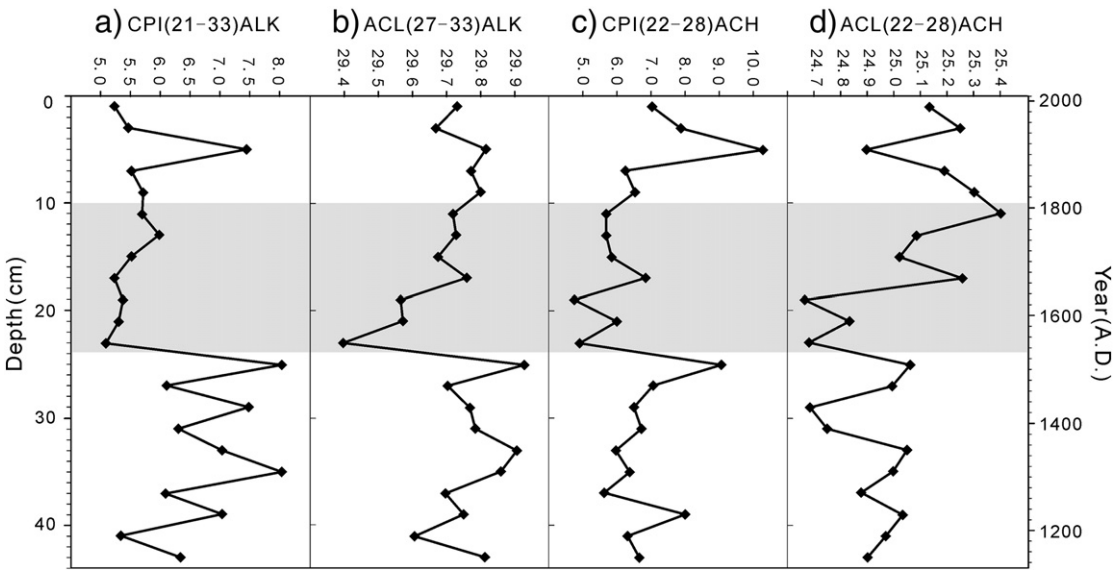

Fig. 7. Carbon preference index (*CPI*) and average chain length (*ACL*) profiles of *n*-alkan-ols (ACH) and *n*-alkanes (ALK) in Core XMC-6. $CPI(21–33)ALK = (C_{21} + 2 \times C_{23} + 2 \times C_{25} + 2 \times C_{27} + 2 \times C_{29} + 2 \times C_{31} + C_{33})/(2 \times \sum C_{22–32}(\text{even}))$; $ACL(27–33)ALK = (27 \times C_{27} + 29 \times C_{29} + 31 \times C_{31} + 33 \times C_{33})/\sum C_{27–33}(\text{odd})$. $CPI(22–28)ACH = 2 \times \sum C_{22–28}(\text{even})/(C_{21} + 2 \times C_{23} + 2 \times C_{25} + 2 \times C_{27} + C_{29})$; $ACL(22–28)ACH = (22 \times C_{22} + 24 \times C_{24} + 26 \times C_{26} + 28 \times C_{28})/\sum C_{22–28}(\text{even})$.

aquatic organisms and allochthonous terrestrial plants contribute to the organic matter in Lake Ximencuo.

4.2. Concentrations of C_{org} and N_{tot} as paleoprecipitation proxies

In lake sediments, organic carbon is derived from multiple sources (aquatic, bacterial and terrestrial), and the concentration of C_{org} reflects both the initial production of biomass as well as subsequent degradation (Meyers, 2003). In some recent studies, the $\%C_{org}$ is considered to be correlated with the precipitation signals in a region. For example, Castañeda et al. (2011) found that $\%C_{org}$ variation in Lake Malawi sediments in east Africa exhibits some coherence with lake level fluctuations over the last 700 yr. Also, variation of the $\%C_{org}$ in sediments deposited over last 18.4 kyr in Lake Donggi Cona is consistent with other paleoprecipitation records from the NE Tibetan Plateau, and short-term drops of $\%C_{org}$ can possibly be related to times of decreased aquatic productivity, which indicate relatively dry episodes (Aichner et al., 2012). The concentration of N_{tot} in lake sediments can also indicate a lake's trophic condition because N exists as proteins, peptides and amino acids, which are the decomposition products from phytoplankton, bacteria and higher plants (Baxby et al., 1994). The annual mean precipitation covering the last 1000 yr has been reconstructed from juniper tree-rings in nearby Dulan (36°17.46′ N, 98°4.44′ E, 3200 m asl, Fig. 1), northeastern QTP and is believed to control the soil effective moisture (Sheppard et al., 2004). The general trend of the tree-ring precipitation history at Dulan appears to be comparable with $\%C_{org}$ and $\%N_{tot}$ in Ximencuo Lake (Fig. 8). When the variations in $\%C_{org}$ and $\%N_{tot}$ are plotted as deviations from a linear fit, the coherence becomes even more apparent. Precipitation seems to be one of the dominant influences on primary productivity in Lake Ximencuo, and thus we postulate that $\%C_{org}$ and $\%N_{tot}$ reflect past precipitation fluctuations in the catchment. The higher $\%C_{org}$ and $\%N_{tot}$ indicate relatively wetter climatic conditions and vice versa. As mentioned above, the relatively higher C_{org}/N_{tot} ratio and lower $\%C_{org}$ and $\%N_{tot}$ at 6–9 cm in Core XMC-5 might document a spell of comparatively dry condition (Fig. 3). One possible factor in this relation is that lower water levels owing to dry climate would make the coring location closer to shore, and it would receive more organic matter from lakeshore plants and consequently the C_{org}/N_{tot} ratio would increase. Another is that drier conditions in the catchment would deliver fewer soil-derived nutrients to the lake, lead to a primary productivity decrease, and result in the lower $\%C_{org}$ and $\%N_{tot}$ associated with the elevated C_{org}/N_{tot} ratios. However, other results from Lake Ximencuo have suggested that variations in the C_{org} concentration probably reflect productivity changes that are

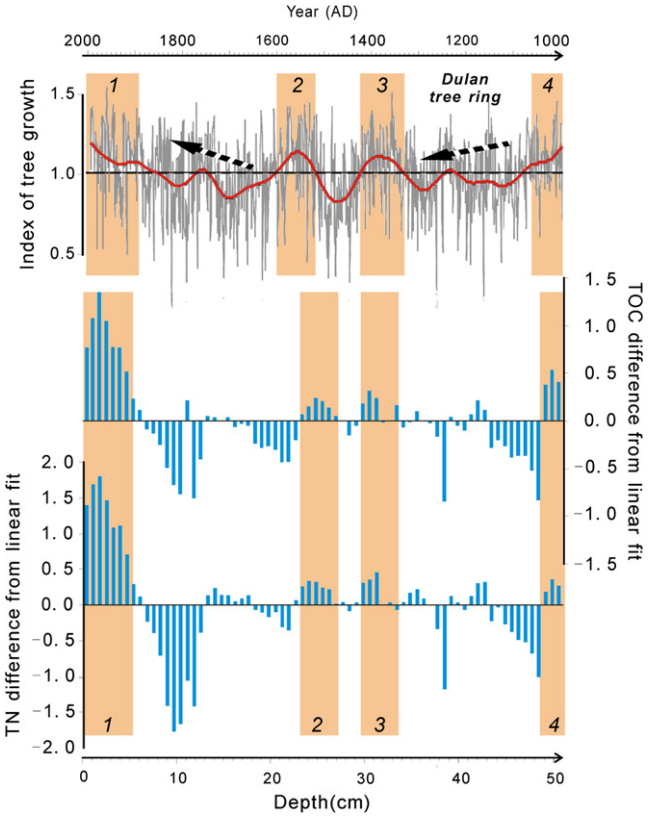

Fig. 8. Concentrations of C_{org} and N_{tot} in Core XMC-5 plotted as the deviation from a linear fit and compared them to the Dulan tree ring series (Sheppard et al., 2004). The dashed-arrows show the overall trend of the tree ring proxy, implying that all the proxies in this figure have similar trends.

mainly controlled by air temperature fluctuations (Mischke and Zhang, 2010). These contrasting interpretations are based on different timescales, which are likely to be important to their differences. The time series of Mischke and Zhang (2010) is about 13.5 kyr BP, and our record extends only to 1 kyr BP. We postulate that the discrepancies between the air temperature and the precipitation variation interpretations will become smaller on longer timescales, especially for climate that is influenced by the Asian Summer Monsoon.

4.3. $\delta^{13}C_{org}$, $\delta^{15}N_{tot}$, CPI and ACL correlations with air temperature variations

The carbon isotopic composition of bulk organic matter in lake sediments can be used as a proxy for past variations in temperature and aquatic productivity, with less negative $\delta^{13}C_{org}$ values generally indicating warm climate and increased aquatic productivity and vice versa (e.g. Hollander and McKenzie, 1991; Saurer et al., 1995). However, the QTP lakes have negative $\delta^{13}C_{org}$ excursions that generally correspond to warm periods, whereas positive excursions are usually related to cold periods, which is contrary to other study areas (e.g. Shen et al., 2005; Xu et al., 2006). One possible explanation for this difference is that more organic matter from land plants was delivered to QTP lake sediments by stronger weathering in warm/humid periods (e.g. Xu et al., 2006). Another is that higher ambient temperatures promoted the photosynthesis of C_3 plants around the lake, which produced more ^{13}C-depleted organic carbon compared to cold conditions (e.g. Smith and Epstein, 1971). For instance, the negative excursions of $\delta^{13}C_{org}$ are inferred to indicate warm conditions with enhanced weathering and vice versa in Lake Qinghai, northeastern QTP (Xu et al., 2006). Moreover, a long core collected in the same lake showed a positive $\delta^{13}C_{org}$ excursion during the Last Glacial Maximum, a period of a cold climate, and a negative shift during the late Holocene, which has been a warmer and wetter period (Shen et al., 2005). In Lake Ximencuo, we hypothesize that the variations of $\delta^{13}C_{org}$ mainly respond to changes in organic matter sources in this hydrologically open, freshwater lake. The postulated increase in C_3 plant biomass and catchment weathering rate during a warm climate can lead to more C_3 plant remains entering the lake sediments by surface runoff, consequently resulting in negative shifts of $\delta^{13}C_{org}$ values and vice versa.

Unlike $\delta^{13}C_{org}$ values, $\delta^{15}N$ is not commonly applied to reconstruct paleoclimate changes in lacustrine sediments because the reasons for $\delta^{15}N$ variations are complicated and are commonly influenced by multiple biogeochemical processes (Hodell and Schelske, 1998; Lu et al., 2010). However, a positive linkage between temperatures and $\delta^{15}N$ has been reported in the surface sediments of Lake Qinghai. Photosynthesis of aquatic plants appears to have played a significant role in determining the $\delta^{15}N$ of organic matter in this lake (Xu et al., 2006). The warm climate helped to promote the photosynthesis of some algae, increased the overall primary productivity in lake, and $\delta^{15}N$ in lake sediments became lower. Conversely, cold climate decreased algal photosynthesis, which resulted in the $\delta^{15}N$ values becoming larger. The profile trend of $\delta^{15}N_{tot}$ is generally in agreement with the $\delta^{13}C_{org}$ in Lake Ximencuo (Fig. 9), suggesting that the $\delta^{15}N_{tot}$ variability seems to be influenced by the same factors that drive $\delta^{13}C_{org}$ variations. Accordingly, we assume that organic matter source variations are responsible for the $\delta^{15}N_{tot}$ changes in Lake Ximencuo. In general, falling or low $\delta^{13}C_{org}$ and $\delta^{15}N_{tot}$ values are interpreted as reflecting warm climatic conditions that are especially favorable for local biomass growth in such high-cold regions.

Changes in the $CPI_{21-33ALK}$, $CPI_{22-28ACH}$ and $ACL_{27-33ALK}$ values are inversely correlated with the $\delta^{13}C_{org}$ and $\delta^{15}N_{tot}$ variations, as indicated by the five shaded zones in Fig. 9. The high *CPI* values of *n*-alkanes and *n*-alkan-ols might indicate a warm climate and vice versa. The consistency between the two types of proxies implies that climate change left an imprint not only on the bulk organic matter but also

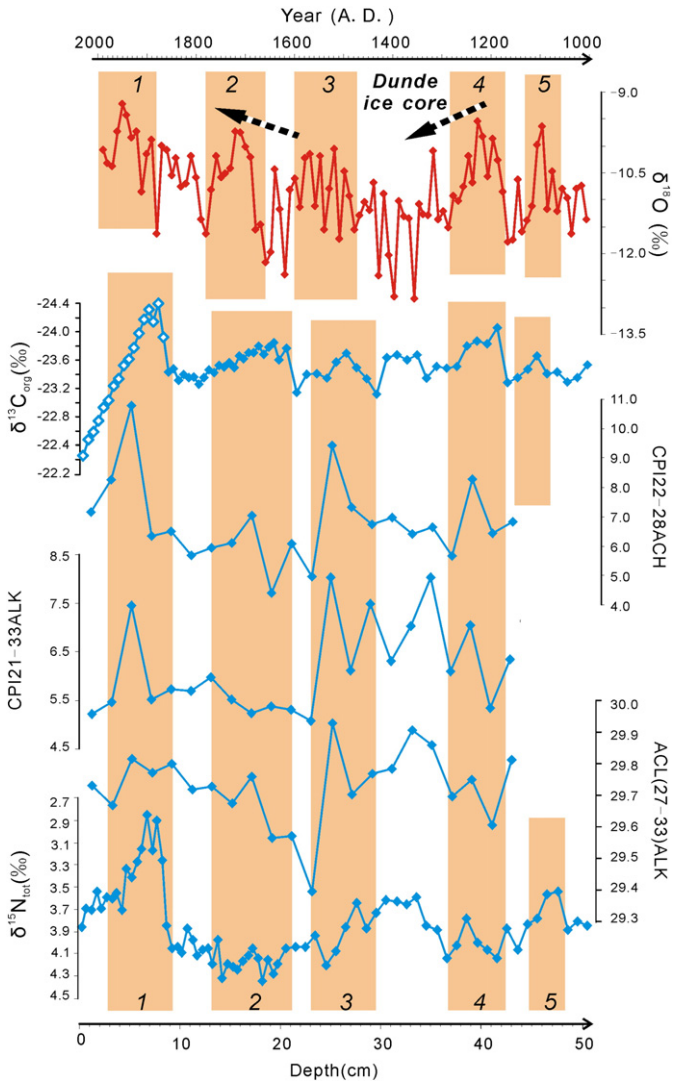

Fig. 9. Comparison between the bulk organic matter isotopic proxies ($\delta^{13}C_{org}$ and $\delta^{15}N_{tot}$) in Core XMC-5 and the lipid biomarker proxies ($CPI_{22-28ACH}$, $CPI_{21-33ALK}$, $ACL_{27-33ALK}$) in Core XMC-6 and the Dunde ice core records in the northeastern part of QTP (Thompson et al., 2003). Open diamonds in the $\delta^{13}C_{org}$ curve indicate the Suess Effect corrections since AD 1840. Shaded bars represent relatively warm climate periods as indicated by the indices. The dashed-arrows show the overall trend of the $\delta^{18}O$ proxy, implying that all the proxies in this figure have similar trends.

on the lipid biomarkers. It should be pointed out that the phase difference between the bulk organic indices and biomarker indices is likely caused by the different sampling resolutions of the bulk and molecular parameters; the overall trends are comparable. Furthermore, the bulk organic matter integrates the information from all organisms living in the lake ecosystem, whereas the $CPI_{21-33ALK}$, $CPI_{22-28ACH}$, and $ACL_{27-33ALK}$ proxies presented in this study indicate the contributions from only vascular higher plants.

The climatic implication of the variations in $CPI_{21-33ALK}$, $CPI_{22-28ACH}$ and $ACL_{27-33ALK}$ can be further assessed by comparing the Lake Ximencuo record with the ice-core oxygen-isotope record over the last 1000 yr at 10-yr time resolution from the Dunde icecap (38°06′ N, 96°24′ E, 5325 m asl, Fig. 1), located in the northeastern QTP (Thompson et al., 2003). The oxygen isotopes in Dunde ice-core are interpreted to reflect large-magnitude shifts in regional temperature, especially responses to summer temperature (Thompson et al., 2003). Also Yang et al. (2010) observed that $\delta^{18}O$ shifts coincide with the percentages of total steppe and meadow pollen in the Puruogangri ice core,

central QTP. Because the steppe and meadow pollen records in the ice core show a significant correlation with the mean summer temperature (e.g. Liu et al., 1998; Herzschuh, 2006; Herzschuh et al., 2006; Yang et al., 2008), it is suggested that the $\delta^{18}O$ record in the Dunde ice core is closely associated with mean temperature variations from June to August, which is the growing season in this high-cold region, and the higher $\delta^{18}O$ values indicate warm periods while the lower $\delta^{18}O$ values are related to relatively cold periods. As shown in Fig. 9, changes in the Ximencuo *CPI* proxies and the nitrogen and carbon isotopic values are comparable with the $\delta^{18}O$ record in the Dunde ice core, particularly with five oxygen isotope positive shifts that are coincident with rising or high *CPI* and *ACL* values (shaded parts in Fig. 9) that indicate comparatively warm periods. The consistencies between the organic proxies in the XMC-5 and XMC-6 cores and the $\delta^{18}O$-temperature in the Dunde ice core suggest that temperature change influences ecosystem development around Lake Ximencuo. In detail, the *CPI* and *ACL* proxies, which are related to physiological processes of the vascular plants, are linked with the $\delta^{18}O$ ice core record, and they imply that temperature has a significant influence on plant growth in this high-cold region. Meanwhile, comparable trends seen in the carbon and nitrogen isotope values and ice core $\delta^{18}O$ variations indicate that the changes in bulk organic matter are also correlated with the climate conditions; warm conditions probably encouraged C_3 plants to flourish in the catchment ecosystem and also promoted photosynthesis of algae and increased the primary productivity in Lake Ximencuo, resulting in the negative excursion of the $\delta^{13}C_{org}$ values and decrease of $\delta^{15}N_{tot}$ values and vice versa.

We must acknowledge that our interpretations of the *CPI* proxies are contrary to those from some studies of peat and modern soil. In example from Northern England, increases in *CPI* values of *n*-alkanes and *n*-alkanoic acids are coincident with lower mean summer temperatures (Xie et al., 2004). In the Hani peat sequence of northeastern China, increases in *CPI* values were similarly interpreted to record cold conditions in the postglacial stage and decreases in *CPI* values of the *n*-alkan-ols to indicate a warming trend in the Holocene (Zhou et al., 2010). In their study of a peat sequence in Spain, Ortiz et al. (2010) also suggested that the lower *n*-alkane *CPI* values could be related to higher degradation rates during warm periods. Finally, the CPI_{23-33} of *n*-alkanes extracted from 62 surface soil samples in eastern China gradually increase with increasing latitudes, a pattern that corresponds to decreasing temperature and precipitation (Rao et al., 2009). The usual explanation for the peat and modern soil *CPI* patterns is that under a cold/arid climate, microbial degradation and diagenesis of organic matter are comparatively slow, preserving the larger *CPI* values of the plant lipids. In contrast, low *CPI* values are evidence of amplified microbial degradation and alteration of organic matter, which are encouraged in a comparatively warmer and wetter climatic setting.

In general, the role of microbial degradation is important to the interpretations of the *CPI* in peat and modern soils in previous studies. However, the situation may be totally different in a glacial lake environment like Ximencuo because annual water temperature shifts in the hypolimnion are likely to be smaller than on land. Therefore, biomarkers in the deep parts of a glacial lake should have good preservation, and the changes in summer temperatures might play only a minor role in lipid degradation. At the same time, the steep terrain around Lake Ximencuo could facilitate rapid runoff that carries organic matter into the lake and thus minimize potential alterations during transport and sedimentation. Finally, vegetation in the Lake Ximencuo catchment is dominated by alpine meadows with dwarf shrubs and without any evidence of significant alteration in plant compositions for at least the last 1000 yr (Yang, 1996; Schlütz and Lehmkuhl, 2009). It is therefore likely that the amount of *CPI* variation resulting from floral change is also minor.

To try to understand the seemingly contradictory interpretation of the Ximencuo *CPI* values, additional factors need to be taken into account. For example, vascular plants biosynthesize longer chain compounds for their waxy coatings under warmer conditions; this response is likely to increase the proportions of odd-carbon *n*-alkanes from C_{21} to C_{33} and even-carbon *n*-alkan-ol components from C_{22} to C_{28} that are produced by higher plants. We postulate that the *CPI* values of waxy lipids of plants that grew in past periods of warm climate would have been larger than those from plants during a cooler climate. This assumption is supported by results from studies of modern tree leaves. The *ACL* values of leaf wax *n*-alkanes show a remarkable seasonal variation, the values of the plant leaves are greater in summer than in spring and autumn, and the highest temperature in August is associated with the largest *ACL* value (Cui et al., 2008). The *n*-alkane *ACL* and *CPI* values of herb and tree leaves from south to north China, which correspond to higher and lower mean annual temperatures, exhibit decreasing trends that are considered to result from the temperature differences (Duan et al., 2011). Also, *CPI* values in lake surface sediments increase slightly along a north to south European transect corresponding to a transition from cold to warm regions (Sachse et al., 2004). These findings serve as a reminder that the *CPI* values would also be influenced by the temperature factor. In the case of Lake Ximencuo, heat and precipitation are adequate for plants to grow efficiently during the growing seasons from May to October (Schlütz and Lehmkuhl, 2009). In warm periods, longer growing seasons probably resulted in higher *CPI* values for the subaerial vascular plants than in cold years, while the intensified surface weathering active via wind and/or runoff in warm periods would facilitate transport of terrestrial lipids with higher *CPI* values to the lake. Hence, it is possible that both a physiological increase of *CPI* values of waxy lipids in vascular plants and an increased influx of vascular detritus entering the lake occur in warm periods. Therefore, sediments with high *CPI* values, as shown in Fig. 9, indicate warm periods, whereas lower *CPI* values are related to relatively cold periods. Moreover, in the alpine meadow ecosystem of Lake Ximencuo, low temperatures combined with frozen surface lake water in the winter season not only inhibit the growth of organisms but also would prevent allochthonous materials from entering the lake. However, more abundant heat and precipitation in the warm-period growing seasons would allow plants to grow more efficiently. Hence, we postulate that the *CPI* values of *n*-alkanes and *n*-alkan-ols in the Ximencuo Lake sediments reflect paleotemperature variations in the growing season from May to October. Although this possible explanation contrasts with *CPI* interpretation proposed in peat and modern soil studies, a few other reports using the *CPI* index in paleoenvironmental reconstructions in lake sediments have hinted at this interpretation. For example, the sedimentary *n*-alkanes extracted from a Lake Baikal core spanning the last 20 kyr showed that the highest CPI_{27-33} values appeared in the Holocene warm period (Brincat et al., 2000). A similar pattern was also observed in Sacred Lake, Kenya, which is a high-altitude freshwater lake in East Africa (Huang et al., 1999). In addition, the sedimentary record from Lake Malawi, southeast Africa, showed that higher *CPI* values are always associated with warm/wet periods that correspond to higher mass accumulation rates of biogenic silica, suggesting increased transport of higher plant leaf waxes to the lake during periods of increased northerly winds and greater productivity (Castañeda et al., 2009).

4.4. Lake Ximencuo paleoclimate reconstruction for the past 1000 yr

By comparing the elemental, isotopic, and molecular organic matter proxies from the sediment record of glacial Lake Ximencuo, the tree ring precipitation record from Dulan (Fig. 8), and the $\delta^{18}O$ temperature record from the Dunde ice core (Fig. 9), the climatic conditions in the Lake Ximencuo catchment of the past 1000 yr can be divided into three stages. Because the XMC-5 and XMC-6 cores have different sampling resolutions, the bulk organic matter and biomarker proxies are not completely concordant. However, the apparent discordance is

small and does not markedly impact the following reconstruction of the paleoclimatic and paleoenvironmental variations:

Stage 1 Before about AD 1550 (core base to 24 cm): the $CPI_{21-33ALK}$, $CPI_{22-28ACH}$, and the $ACL_{27-33ALK}$ values have overall high values, although with some small fluctuations (Figs. 7 and 9), implying comparatively warm conditions in this period, which corresponds to the *MWP*. Precipitation was higher initially, as indicated by elevated $\%C_{org}$ and $\%N_{tot}$ (Fig. 8), and then apparently diminished (low concentrations) before gradually rising again to above average values, and finally was followed by moderately dry conditions near the end of this period as implied by lower concentrations of C_{org} and N_{tot}.

Stage 2 From around AD 1550 to 1850 (24 cm to 10 cm), a cold event first abruptly terminated the *MWP*, and then climate slowly moderated but remained cool (Figs. 7 and 9). This cold period centered on the 17th century roughly corresponds in time to the *LIA*, which has also been identified in other paleotemperature records from the QTP (e.g. Yao et al., 1997; Liu et al., 2011 and references therein). Higher values of %TOC and %TN indicate relatively higher paleoprecipitation that suggests that the early part of the *LIA* was comparatively wet in this region. However, from AD 1760 to 1850, precipitation apparently decreased, as indicated by the lowest $\%C_{org}$ and $\%N_{tot}$ values in the whole sedimentary sequence, suggesting that a cold and dry climate prevailed in the latter part of the *LIA*.

Stage 3 From about AD 1850 to the present (10 cm to core top), the climate was generally warmer than during the earlier stages, which might correspond to the period of the *MW*. However, the temperature on the QTP was unstable during the past 150 yr (Figs. 7 and 9). From relatively high initial values, it has tended to decrease in recent century, which is evident in the $\delta^{13}C_{org}$, $\delta^{15}N_{tot}$ and *CPI* indexes in Lake Ximencuo and in the Dunde $\delta^{18}O$-temperature record, as shown in Fig. 9. It seems that the warmest spell on the eastern QTP after the *LIA* was not in recent decades, but mostly in the early and middle twentieth century. This conclusion is supported by the annual mean temperature variation from 1880 to 2003 in QTP that has been reconstructed from meteorological data and tree-rings (Wang et al., 2004). However, precipitation likely has continued to rise for the past 150 yr.

In general, the air temperature variation is out-of-phase with the precipitation variation. In particular, the four shaded intervals in Fig. 8 that indicate the wet periods are not concordant with the five shaded intervals in Fig. 9 that indicate warm periods for the past 1000 yr. Also, it is hard to conclude whether air temperature and precipitation exist in either a phase-lead or a phase-lag relation. However, we can hypothesize as to why air temperature and precipitation in the Lake Ximencuo record show different variations at the centennial-scale or even multi-centennial-scale. On the basis of the previous studies, the QTP can be roughly divided into three circulation zones according to the influences of atmospheric circulation: the monsoon zone (south of 30° N), the transition zone (between 30° and 35° N), and the Westerly zone (north of 35° N). Climate is generally believed to be characterized by warm-wet or cold-dry combinations in the region that is controlled by the Asian Summer Monsoon rains (An, 2000; Wang et al., 2005). This situation means that temperature and precipitation variations are usually synchronized in the monsoonal areas. However, air temperature variations in the mid-latitude Westerly region are significantly different from precipitation variations. For example, the precipitation trend reconstructed from the glacial accumulation rate apparently lags behind the temperature variation that is deduced from the $\delta^{18}O$ record in the Guliya ice core, northwest QTP (Yao et al., 1996). Furthermore, based on various paleoclimate archives, such as ice cores, tree rings, and lake sediments, Yang et al. (2009) concluded that temperature and precipitation show significant negative correlations on annual, decadal, centennial and even millennial timescales in mid-latitude arid central Asia. Likewise, wet *LIA* conditions and dry *MWP* conditions have been reconstructed in the Westerly-dominated regions of Asia by recent studies (e.g. Chen et al., 2010; Liu et al., 2011). This hydrologic–thermal combination could be potentially explained by changes in the trajectory or strength of the Westerlies (Chen et al., 2010), the topographic features in this area (Herzschuh, 2006; Herzschuh et al., 2006), or both, as the previous studies summarized. Lake Ximencuo is located in the transitional zone that should sensitively reflect the spatial expansion or contraction of the dominating circulation systems during the last 1000 yr because of its marginal position in relation to both the summer monsoon and the Westerlies. A possible mechanism is that when the Asia Summer Monsoon intensifies, precipitation in Lake Ximencuo catchment is mainly derived from the Indian Ocean and the Western Pacific, and when the Asia Monsoon weakens, the Westerlies would move southward and bring moisture from the North Atlantic. However, the Westerly winds also became agents for drier conditions on their way to the eastern QTP due to the loss of moisture along their long travel path. This importance of this factor would depend on the wind strength and the amount of water vapor transported by the Westerlies from the North Atlantic. On the other hand, a previous study has shown that the temperature changes in central Asia were comparable with Northern Hemisphere temperature changes over the last millennium (Treydte et al., 2006). Furthermore, air temperature variations in the eastern QTP could be also ascribed to changes in solar insolation, volcanism, and greenhouse gas concentration (Hegerl et al., 2003), which show the same pace with regional temperature variation that are implied by fluctuations in the Dunde $\delta^{18}O$ ice-core record (Fig. 9).

Previous studies have demonstrated that the eastern QTP has been mainly influenced by Asian Summer Monsoons during the Holocene (e.g. Zhang and Mischke, 2009; Zhao et al., 2011), yet influences from the Westerlies are rarely mentioned. Actually, the dotted arrows used in Figs. 8 and 9 to illustrate that the air temperature and precipitation proxies first declined and then strongly increased indicate that the air temperature and precipitation have comparable trends in the Lake Ximencuo catchment for the last 1000 yr. Thus, we conclude that the regional air temperature and precipitation variations are synchronized in the eastern QTP at a millennial or perhaps even a larger scale, which is an expression of the Asian Summer Monsoon signals but not of the Westerly signals. A reasonable interpretation is that the climate in the eastern QTP is driven more by the Asian Summer Monsoon than by the Westerlies, even if the QTP is located in the transitional zone. The complex mechanism that drives climate evolution at the comparatively short time scale could become less important when the time scale enlarges. This phenomenon could be clearly observed in large time scale studies (e.g. Zhang and Mischke, 2009; Zhao et al., 2011). In conclusion, the relation between the air temperature and the precipitation might be ambiguous in short time scales, such as centennial or even multi-centennial, but in the millennial or even larger time scales, air temperature and precipitation present matched trends in the eastern QTP, which is located in the transitional zone between the Asian Monsoon region and the Westerlies region. The time scale is clearly an important factor to be considered for discussions of paleoclimatic variations.

5. Conclusions

We have used measurements of the bulk organic matter concentrations and isotopic compositions and the distributions of *n*-alkane and *n*-alkan-ol biomarkers in two sister cores from Lake Ximencuo on the Qinghai–Tibetan Plateau to reconstruct a 1 kyr record of

regional climate change. Variations in these paleoclimate proxies lead to these conclusions:

(1) The $\delta^{13}C_{org}$, $\delta^{15}N_{tot}$ and atomic C_{org}/N_{tot} ratio enable us to identify the origin of the organic matter in Lake Ximencuo sediments, whereas the lipid biomarker distribution patterns indicate the origin of only the lipid components. The bulk organic matter in these lake sediments originates from a mixed source comprising autochthonous algae and aquatic and terrestrial plant inputs, and the *n*-alkanes and *n*-alkan-ols mainly originate from vascular higher plants around the lake. Contradictory source indications between the elemental and carbon isotopic proxies in the recent century show that the Suess Effect should be taken into account in Lake Ximencuo.

(2) Variations of $\delta^{13}C_{org}$ and $\delta^{15}N_{tot}$ values correspond in time with those of the $CPI_{22-28ACH}$ and $CPI_{22-33ALK}$ proxies, but they exhibit negative correlations. The higher *CPI* values of the higher-plant-derived components are likely related to warm conditions with enhanced wash-in of plant debris to the lake, whereas lower values correspond to cold conditions and diminished wash-in. This interpretation contrasts with those from peat and soil studies. Differences between the depositional environments and their organic matter sources, as well as the physiological responses of higher plants to changing climatic conditions, are probably responsible for the differing explanations.

(3) Changes in the concentrations of C_{org} and N_{tot} in the sediments of Lake Ximencuo correlate positively with the tree-ring precipitation record in Dulan, and thus they are believed to be reliable proxies for past precipitation in this region. Increases in the C_{org} and N_{tot} concentrations indicate periods of wetter climate during the Medieval Warm Period and since the Little Ice Age. Decreases in this proxy indicate times of less wet climate near the ends of the Medieval Warm Period and the Little Ice Age.

(4) The paleoclimate data and organic proxies used in this study provide a general overview of the climate changes associated with environmental variations in the Lake Ximencuo area during the past millennium. In general, variations in the *CPI* values of *n*-alkan-ols and *n*-alkanes, the *ACL* values of *n*-alkanes, and the $\delta^{13}C_{org}$ and $\delta^{15}N_{tot}$ proxies are inferred to record air temperature variations in the growing season in Lake Ximencuo area; these variations are comparable with those in the Dunde ice core $\delta^{18}O$ paleotemperature record.

(5) Changes in air temperature do not always correspond with changes in the precipitation in the eastern QTP on a centennial-scale or even multi-centennial-scale. This inconsistency could be partly because Lake Ximencuo is located in the transitional zone between the Asian Monsoon and the Westerlies. The precipitation of the eastern QTP may be influenced not only by monsoonal circulation but also the Westerlies. However, air temperature might respond to additional factors such as variations in solar insolation, volcanic eruptions and greenhouse gas concentrations, which is consistent with the regional climatic change. Consequently, the apparent inconsistency between air temperature and precipitation variations will probably become less on longer timescales.

Acknowledgments

We thank Prof. Shijie Li, Drs. Wei Chen, Hezhong Yuan and Yongjian Jiang for taking part in the fieldwork and sample collection. We also appreciate the support for the laboratory work from Prof. Junhua Huang, Drs. Xianyu Huang, Canfa Wang and Jingjing Li in the State Key Laboratory of Geological Processes and Mineral Resources, China University of Geosciences. This work was supported by the Major State Basic Research Development Program of China (Grant No. 2012CB214701) and the Chinese Academy of Sciences Key Project (Grant No. XDB03020405), the National Natural Science Foundation of China (Grant No. 40871096). We thank two anonymous reviewers for their thoughtful and constructive comments that greatly helped us to improve this manuscript.

Appendix A. Supplementary data

Supplementary data associated with this article can be found in the online version, at http://dx.doi.org/10.1016/j.palaeo.2013.03.023. These data include Google map of the most important areas described in this article.

References

Aichner, B., Herzschuh, U., Wilkes, H., Schulz, H.-M., Wang, Y., Plessen, B., Mischke, S., Diekmann, B., Zhang, C., 2012. Ecological development of Lake Donggi Cona, north-eastern Tibetan Plateau, since the late glacial on basis of organic geochemical proxies and non-pollen palynomorphs. Palaeogeography, Palaeoclimatology, Palaeoecology 313–314, 140–149.

An, Z.S., 2000. The history and variability of the East Asian paleomonsoon climate. Quaternary Science Reviews 19, 171–187.

An, Z.S., Kutzbach, J.E., Prell, W.L., Porter, S.C., 2001. Evolution of Asian monsoons and phased uplift of the Himalaya–Tibetan plateau since Late Miocene times. Nature 411, 62–66.

Appleby, P.G., Oldfield, F., 1992. Application of Pb-210 to sedimentation studies. In: Ivanovich, M., Harmon, R.S. (Eds.), Uranium-series Disequilibrium: Applications to Earth, Marine, and Environmental Problems. Clarendon Press, Oxford, pp. 731–778.

Baxby, M., Patience, R.L., Bartle, K.D., 1994. The origin and diagenesis of sedimentary organic nitrogen. Journal of Petroleum Geology 17, 211–230.

Brincat, D., Yamada, K., Ishiwatari, R., Uemura, H., Naraoka, H., 2000. Molecular-isotopic stratigraphy of long-chain n-alkanes in Lake Baikal Holocene and glacial age sediments. Organic Geochemistry 31, 287–294.

Calvert, S.E., 2004. Beware intercepts: interpreting compositional ratios in multi-component sediments and sedimentary rocks. Organic Geochemistry 35, 981–987.

Castañeda, I.S., Werne, J.P., Johnson, T.C., Filley, T.R., 2009. Late Quaternary vegetation history of southeast Africa: the molecular isotopic record from Lake Malawi. Palaeogeography, Palaeoclimatology, Palaeoecology 275, 100–112.

Castañeda, I.S., Werne, J.P., Johnson, T.C., Powers, L.A., 2011. Organic geochemical records from Lake Malawi (East Africa) of the last 700 years, part II: biomarker evidence for recent changes in primary productivity. Palaeogeography, Palaeoclimatology, Palaeoecology 303, 140–154.

Chen, F.H., Chen, J.H., Holmes, J., Boomer, I., Austin, P., Gates, J.B., Wang, N.L., Brooks, S.J., Zhang, J.W., 2010. Moisture changes over the last millennium in arid central Asia: a review, synthesis and comparison with monsoon region. Quaternary Science Reviews 29, 1055–1068.

China meteorological data sharing service system http://data.cma.gov.cn.

Cranwell, P.A., Eglinton, G., Robinson, N., 1987. Lipids of aquatic organisms as potential contributors to lacustrine sediments-II. Organic Geochemistry 11, 513–527.

Cui, J.W., Huang, J.H., Xie, S.C., 2008. Characteristics of seasonal variations of leaf *n*-alkanes and *n*-alkenes in modern higher plants in Qingjiang, Hubei Province, China. Chinese Science Bulletin 53, 2659–2664.

Duan, Y., Wu, B.X., Xu, L., Zhang, X.L., He, J.X., 2011. Compositions of *n*-alkanes and their isotopes in plants from the different latitude regions in China. Acta Geologica Sinica 85, 262–271 (in Chinese with English abstract).

Eglinton, T.I., Eglinton, G., 2008. Molecular proxies for paleoclimatology. Earth and Planetary Science Letters 275, 1–16.

Eglinton, G., Hamilton, R.J., 1967. Leaf epicuticular waxes. Science 156, 1322–1335.

Farquhar, G.D., Ehleringer, J.R., Hubick, K.T., 1989. Carbon isotope discrimination and photosynthesis. Annual Review of Plant Physiology and Plant Molecular Biology 40, 503–537.

Ficken, K.J., Barber, K.E., Eglinton, G., 1998. Lipid biomarker, $\delta^{13}C$ and plant macrofossil stratigraphy of a Scottish montane peat bog over the last two millennia. Organic Geochemistry 28, 217–237.

Ficken, K.J., Li, B., Swain, D.L., Eglinton, G., 2000. An *n*-alkane proxy for the sedimentary input of submerged/floating freshwater aquatic macrophytes. Organic Geochemistry 31, 745–749.

Hegerl, G.C., Crowley, T.J., Baum, S.K., Kim, K.-Y., Hyde, W.T., 2003. Detection of volcanic, solar and greenhouse gas signals in paleo-reconstructions of Northern Hemispheric temperature. Geophysical Research Letters 30 (46-1–46-4).

Henderson, A.C.G., Holmes, J.A., 2009. Palaeolimnological evidence for environmental change over the past millennium from Lake Qinghai sediments: a review and future research prospective. Quaternary International 194, 134–147.

Herzschuh, U., 2006. Palaeo-moisture evolution in monsoonal Central Asia during the last 50,000 years. Quaternary Science Reviews 25, 163–178.

Herzschuh, U., Zhang, C., Mischke, S., Herzschuh, R., Mohammadi, F., Mingram, B., Krschner, H., Riedel, F., 2005. A late Quaternary lake record from the Qilian Mountains (NW China): evolution of the primary production and the water depth reconstructed from macrofossil, pollen, biomarker, and isotope data. Global and Planetary Change 46, 361–379.

Herzschuh, U., Winter, K., Wünemann, B., Li, S., 2006. A general cooling trend on the central Tibetan Plateau throughout the Holocene recorded by the Lake Zigetang pollen spectra. Quaternary International 154–155, 113–121.
Hodell, D.A., Schelske, C.L., 1998. Production, sedimentation, and isotopic composition of organic matter in Lake Ontario. Limnology and Oceanography 43, 200–214.
Hollander, D.J., McKenzie, J.A., 1991. CO_2 control on carbon-isotope fractionation during aqueous photosynthesis: a paleo-pCO_2 barometer. Geology 19, 929–932.
Huang, Y., Street-Perrott, F.A., Perrott, R.A., Metzger, P., Eglinton, G., 1999. Glacial–interglacial environmental changes inferred from molecular and compound-specific $\delta^{13}C$ analyses of sediments from Sacred Lake, Mt. Kenya. Geochimica et Cosmochimica Acta 63, 1383–1404.
Hughen, K.A., Eglinton, T.I., Xu, L., Makou, M., 2004. Abrupt tropical vegetation response to rapid climate changes. Science 304, 1955–1959.
Ji, J.F., Shen, J., Balsam, W., Chen, J., Liu, L.W., Liu, X.Q., 2005. Asian monsoon oscillations in the northeastern Qinghai–Tibet Plateau since the late glacial as interpreted from visible reflectance of Qinghai Lake sediments. Earth and Planetary Science Letters 233, 61–70.
Keeling, C.D., 1979. The Suess effect: ^{13}carbon–^{14}carbon interrelations. Environment International 2, 229–300.
Lehmkuhl, F., 1998. Extent and spatial distribution of Pleistocene glaciations in eastern Tibet. Quaternary International 45–46, 123–134.
Lin, X., Zhu, L.P., Wang, Y., Wang, J.B., Xie, M.P., Ju, J.T., Maubacher, R., Schwalb, A., 2008. Environmental changes reflected by *n*-alkanes of lake core in Nam Co on the Tibetan Plateau since 8.4 ka BP. Chinese Science Bulletin 53, 3051–3057.
Liu, K.B., Yao, Z.J., Thompson, L.G., 1998. A pollen record of Holocene climatic changes from the Dunde ice cap, Qinghai–Tibetan Plateau. Geology 26, 135–138.
Liu, X., Herzschuh, U., Shen, J., Jiang, Q., Xiao, X., 2008. Holocene environmental and climatic changes inferred from Wulungu Lake in northern Xinjiang, China. Quaternary Research 70, 412–425.
Liu, W.G., Liu, Z.H., An, Z.S., Wang, X.L., Chang, H., 2011. Wet climate during the 'Little Ice Age' in the arid Tarim Basin, northwestern China. The Holocene 21, 409–416.
Lu, Y.H., Meyers, P.A., Johengen, T.H., Eadie, B.J., Robbins, J.A., Han, H., 2010. $\delta^{15}N$ values in Lake Erie sediments as indicators of nitrogen biogeochemical dynamics during cultural eutrophication. Chemical Geology 273, 1–7.
Meyers, P.A., 1994. Preservation of elemental and isotopic source identification of sedimentary organic matter. Chemical Geology 114, 289–302.
Meyers, P.A., 1997. Organic geochemical proxies of paleoceanographic, paleolimnologic, and paleoclimatic processes. Organic Geochemistry 27, 213–250.
Meyers, P.A., 2003. Applications of organic geochemistry to paleolimnological reconstructions: a summary of examples from the Laurentian Great Lakes. Organic Geochemistry 34, 261–289.
Meyers, P.A., Lallier-Vergès, E., 1999. Lacustrine sedimentary organic matter records of Late Quaternary paleoclimates. Journal of Paleolimnology 21, 345–372.
Mischke, S., Zhang, C.J., 2010. Holocene cold events on the Tibetan Plateau. Global and Planetary Change 72, 155–163.
Mügler, I., Sachse, D., Werner, M., Xu, B., Wu, G., Yao, T., Gleixner, G., 2008. Effect of lake evaporation on δD values of lacustrine *n*-alkanes: a comparison of Nam Co (Tibetan Plateau) and Holzmaar (Germany). Organic Geochemistry 39, 711–729.
Ortiz, J.E., Gallego, J.L.R., Torres, T., Díaz-Bautista, A., Sierra, C., 2010. Palaeoenvironmental reconstruction of Northern Spain during the last 8000 cal yr BP based on the biomarker content of the Roñanzas peat bog (Asturias). Organic Geochemistry 41, 454–466.
Poynter, J.G., Farrimond, P., Brassell, S.C., Eglinton, G., 1989. Aeolian-derived higher-plant lipids in the marine sedimentary record: links with paleoclimate. In: Leinen, M., Sarnthein, M. (Eds.), Palaeoclimatology and Palaeometeorology: Modern and Past Patterns of Global Atmosphere Transport. Kluwer, pp. 435–462.
Rao, Z.G., Zhu, Z.Y., Wang, S.P., Jia, G.D., Qiang, M.R., Wu, Y., 2009. CPI values of terrestrial higher plant-derived long-chain *n*-alkanes: a potential paleoclimatic proxy. Frontiers of Earth Science in China 3, 266–272.
Robinson, N., Cranwell, P.A., Finlay, B.J., Eglinton, G., 1984. Lipids of aquatic organisms as potential contributors to lacustrine sediments. Organic Geochemistry 6, 143–152.
Rommerskirchen, F., Plader, A., Eglinton, G., Chikaraishi, Y., Rullkötter, J., 2006. Chemotaxonomic significance of distribution and stable carbon isotopic composition of long-chain alkanes and alkan-1-ols in C_4 grass waxes. Organic Geochemistry 37, 1303–1332.
Russell, J.M., McCoy, S.J., Verschuren, D., Bessems, I., Huang, Y., 2009. Human impacts, climate change, and aquatic ecosystem response during the past 2000 yr at Lake Wandakara, Uganda. Quaternary Research 72, 315–324.
Sachse, D., Radke, J., Gleixner, G., 2004. Hydrogen isotope ratios of recent lacustrine sedimentary *n*-alkanes record modern climate variability. Geochimica et Cosmochimica Acta 68, 4877–4889.
Saurer, M., Siegenthaler, U., Schweingruber, F., 1995. The climate–carbon isotope relationship in tree rings and the significance of site conditions. Tellus 47, 320–330.
Schelske, C.L., Hodell, D.A., 1995. Using carbon isotopes of bulk sedimentary organic matter to reconstruct the history of nutrient loading and eutrophication in Lake Erie. Limnology and Oceanography 40, 918–929.
Schlütz, F., Lehmkuhl, F., 2009. Holocene climatic change and the nomadic Anthropocene in Eastern Tibet: palynological and geomorphological results from the Nianbaoyeze Mountains. Quaternary Science Reviews 28, 1449–1471.
Sepúlveda, J., Pantoja, S., Hughen, K.A., Bertrand, S., Figueroa, D., León, T., Drenzek, N.J., Lange, C., 2009. Late Holocene sea-surface temperature and precipitation variability in northern Patagonia, Chile (Jacaf Fjord, 44°S). Quaternary Research 72, 400–409.
Shao, X.M., Huang, L., Liu, H.B., Liang, E.Y., Fang, X.Q., Wang, L.L., 2005. Reconstruction of precipitation variation from tree rings in recent 1000 years in Delingha, Qinghai. Science in China 48, 939–949 (Ser. D).
Shen, Z.L., Zhu, W.H., Zhong, Z., 1993. Basic of Hydrogeochemistry. Geological Press, Beijing (in Chinese).
Shen, J., Liu, X.Q., Wang, S.M., Ryo, M., 2005. Palaeoclimatic changes in the Qinghai Lake area during the last 18,000 years. Quaternary International 136, 131–140.
Sheppard, R.P., Tarasov, E.P., Graumlich, J.L., Heussner, U.K., Wagner, M., Österle, H., Thompson, G.L., 2004. Annual precipitation since 515 BC reconstructed from living and fossil juniper growth of northeastern Qinghai Province, China. Climate Dynamics 23, 869–881.
Smith, B.N., Epstein, S., 1971. Two categories of $^{13}C/^{12}C$ ratios for higher plants. Plant Physiology 47, 380–384.
Thompson, L., Mosley-Thompson, E., Davis, M., Bolzan, J., Dai, J., Klein, L., Yao, T., Wu, X., Xie, Z., Gundestrup, N., 1989. Holocene–Late Pleistocene climatic ice core records from Qinghai–Tibetan Plateau. Science 246, 474–477.
Thompson, L.G., Yao, T., Davis, M.E., Henderson, K.A., Mosley-Thompson, E.P.-N., Lin, J.B., Synal, H.-A., Cole-Dai, J., Bolzan, J.F., 1997. Tropical climate instability: the last glacial cycle from a Qinghai–Tibetan ice core. Science 276, 1821–1825.
Thompson, L.G., Mosley-Thompson, E., Davis, M.E., Lin, P.N., Henderson, K., Mashiotta, T.A., 2003. Tropical glacier and ice core evidence of climate change on annual to millennial time scales. Climatic Change 59, 137–155.
Treydte, K.S., Schleser, G.H., Helle, G., Frank, D.C., Winiger, M., Haug, G.H., Esper, J., 2006. The twentieth century was the wettest period in northern Pakistan over the past millennium. Nature 440, 1179–1182.
Tulloch, A.P., 1976. Chemistry of waxes of higher plants. In: Kolattukudy, P.E. (Ed.), Chemistry and Biochemistry of Natural Waxes. Elsevier, Amsterdam.
Vogts, A., Moossen, H., Rommerskirchen, F., Rullkötter, J., 2009. Distribution patterns and stable carbon isotopic composition of alkanes and alkan-1-ols from plant waxes of African rain forest and savanna C_3 species. Organic Geochemistry 40, 1037–1054.
Volkman, J.K., Barrett, S.M., Blackburn, S.I., Mansour, M.P., Sikes, E.L., Gelin, F., 1998. Microalgal biomarkers: a review of recent research developments. Organic Geochemistry 29, 1163–1179.
Wang, S.M., Dou, H.S., 1998. China Lake Records (in Chinese). Science Press, Beijing.
Wang, S.M., Xue, B., Xia, W.L., 1997. Lake record of climatic change in the past 2000 years of Ximen Cuo (Lake). Quaternary Sciences 17, 62–69 (in Chinese with English abstract).
Wang, S.W., Zhu, J.H., Cai, J.N., 2004. Interdecadal variability of temperature and precipitation in China since 1880. Advances in Atmospheric Sciences 21, 307–313.
Wang, Y.J., Cheng, H., Edwards, R.L., He, Y., Kong, X.G., An, Z.S., Wu, J.Y., Kelly, M.J., Dykoski, C.A., Li, X.D., 2005. The Holocene Asian Monsoon: links to solar changes and North Atlantic climate. Science 308, 854–857.
Wrozyna, C., Frenzel, P., Steeb, P., Zhu, L., Schwalb, A., 2011. Recent lacustrine Ostracoda and a first transfer function for palaeo-water depth estimation in Nam Co, southern Tibetan Plateau. Revista Española de Micropaleontología 41, 1–20.
Wu, Y.H., Lucke, A., Jin, Z.D., Wang, S.M., Schleser, G.H., Battarbee, R.W., Xia, W.L., 2006. Holocene climate development on the central Tibetan Plateau: a sedimentary record from Cuoe Lake. Palaeogeography, Palaeoclimatology, Palaeoecology 234, 328–340.
Wu, Y.H., Lücke, A., Wünnemann, B., LI, S.J., Wang, S.M., 2007. Holocene climate change in the Central Tibetan Plateau inferred by lacustrine sediment geochemical records. Science in China 50, 1548–1555 (Ser. D).
Xie, S., Evershed, R.P., 2001. Peat molecular fossils recording paleoclimatic change and organism replacement. Chinese Science Bulletin 46, 1749–1752.
Xie, S., Nott, C.J., Avsejs, L.A., Maddy, D., Chambers, F.M., Evershed, R.P., 2004. Molecular and isotopic stratigraphy in an ombrotrophic mire for paleoclimate reconstruction. Geochimica et Cosmochimica Acta 68, 2849–2862.
Xu, H., Ai, L., Tan, L.C., An, Z.S., 2006. Stable isotopes in bulk carbonates and organic matter in recent sediments of Lake Qinghai and their climatic implications. Chemical Geology 235, 262–275.
Xu, H., Hou, Z.H., An, Z.S., Liu, X.Y., Dong, J.B., 2010. Major ion chemistry of waters in Lake Qinghai catchments, NE Qinghai–Tibet plateau, China. Quaternary International 212, 35–43.
Xue, B., Pan, H.X., Xia, W.L., Wang, S.M., 1997. Palaeoenvironmental reconstruction of Ximen Cuo in historical period inferred from pigment record. Journal of Lakes Science 9, 295–298 (in Chinese with English abstract).
Yang, X.D., 1996. Pollen assemblage and palaeoclimate during last 2000 year in Ximencuo region, Qinghai. Acta Micropalaeontologica Sinica 13, 437–440 (in Chinese with English abstract).
Yang, B., Tang, L.Y., Bräuning, A., Davis, M.E., Shao, J.J., Liu, J.J., 2008. Summer temperature reconstruction on the central Tibetan Plateau during 1860–2002 derived from annually resolved ice core pollen. Journal of Geophysical Research — Atmospheres 113, D24102.
Yang, B., Wang, J., Bräning, A., Dong, Z., Esper, J., 2009. Late Holocene climatic and environmental changes in arid central Asia. Quaternary International 194, 68–78.
Yang, B., Tang, L.Y., Li, C.H., Shao, Y.J., Tao, S.C., Yang, L.Q., 2010. An ice-core record of vegetation and climate changes in the central Tibetan Plateau during the last 550 years. Chinese Science Bulletin 55, 1169–1177.
Yao, T.D., Thompson, L.G., Qin, D.H., Tian, L.D., Jiao, K.Q., Yang, Z.H., Xie, C., 1996. Variations in temperature and precipitation in the past 2000 a on the Xizang (Tibet) Plateau — Guliya ice core record. Science in China 39, 425–433 (Ser. D).
Yao, T.D., Shi, Y.F., Thompson, L.G., 1997. High resolution record of paleoclimate since the Little Ice Age from the Tibetan ice cores. Quaternary International 37, 19–23.
Zhang, C.J., Mischke, S., 2009. A Lateglacial and Holocene lake record from the Nianbaoyeze Mountains and inferences of lake, glacier and climate evolution on the eastern Tibetan Plateau. Quaternary Science Reviews 28, 1970–1983.
Zhang, Z., Zhao, M., Eglinton, G., Lu, H., Huang, C.-Y., 2006. Leaf wax lipids as paleovegetational and paleoenvironmental proxies for the Chinese Loess Plateau over the last 170 kyr. Quaternary Science Reviews 25, 575–594.
Zhao, Y., Yu, Z., Zhao, W., 2011. Holocene vegetation and climate histories in the eastern Tibetan Plateau: controls by insolation-driven temperature or monsoon-derived precipitation changes? Quaternary Science Reviews 30, 1173–1184.

Zheng, Y.H., Zhou, W.J., Liu, X., Zhang, C.L., 2011a. *n*-Alkan-2-one distributions in a northeastern China peat core spanning the last 16 kyr. Organic Geochemistry 42, 25–30.

Zheng, Y.H., Zhou, W.J., Meyers, P.A., 2011b. Proxy value of *n*-alkan-2-ones in the Hongyuan peat sequence to reconstruct Holocene climate changes on the eastern margin of the Tibetan Plateau. Chemical Geology 288, 97–104.

Zhou, W.J., Zheng, Y.H., Meyers, P.A., Jull, A.J.T., Xie, S.C., 2010. Postglacial climate-change record in biomarker lipid compositions of the Hani peat sequence, Northeastern China. Earth and Planetary Science Letters 294, 37–46.

Zhu, L.P., Wu, Y.H., Wang, J.B., Lin, X., Ju, J.T., Xie, M.P., Li, M.H., Mausbacher, R., Schwalb, A., Daut, G., 2008. Environmental changes since 8.4 ka reflected in the lacustrine core sediments from Nam Co, central Tibetan Plateau, China. The Holocene 18, 831–839.

Zhu, H.F., Shao, X.M., Yin, Z.Y., Xu, P., Xu, Y., Tian, H., 2011. August temperature variability in the southeastern Tibetan Plateau since AD 1385 inferred from tree rings. Palaeogeography Palaeoclimatology Palaeoecology 305, 84–92.